

Effect of obesity and epicardial fat/fatty infiltration on electrical and structural remodeling associated with atrial fibrillation in a novel canine model of obesity and atrial fibrillation: A comparative study

日本大学大学院医学研究博士課程







内科系循環器内科学専攻

大塚 直人

修了年 2023年

指導教員 奥村 恭男

# Effect of obesity and epicardial fat/fatty infiltration on electrical and structural remodeling associated with atrial fibrillation in a novel canine model of obesity and atrial fibrillation: A comparative study

Naoto Otsuka MD<sup>1</sup>  | Yasuo Okumura MD<sup>1</sup>  | Masaru Arai MD<sup>1</sup> |  
 Sayaka Kurokawa MD<sup>1</sup> | Koichi Nagashima MD<sup>1</sup>  | Ryuta Watanabe MD<sup>1</sup> |  
 Yuji Wakamatsu MD<sup>1</sup>  | Seina Yagyu MD<sup>1</sup>  | Kimie Ohkubo MD<sup>1</sup> |  
 Toshiko Nakai MD<sup>1</sup>  | Hiroyuki Hao MD<sup>2</sup> | Rie Takahashi RA<sup>3</sup> |  
 Yoshiki Taniguchi RA<sup>3</sup> | Yxin Li MD<sup>4</sup>

<sup>1</sup>Department of Medicine, Division of Cardiology, Nihon University School of Medicine, Tokyo, Japan

<sup>2</sup>Department of Pathology and Microbiology, Division of Human Pathology, Nihon University School of Medicine, Tokyo, Japan

<sup>3</sup>Institute of Medical Science, Medical Research Support Center, Section of Laboratory for Animal Experiments, Nihon University School of Medicine, Tokyo, Japan

<sup>4</sup>Division of Cell Regeneration and Transplantation, Department of Functional Morphology, Nihon University School of Medicine, Tokyo, Japan

## Correspondence

Yasuo Okumura, MD, Division of Cardiology, Department of Medicine, Nihon University School of Medicine, Ohyaguchi-kamicho, Itabashi-ku, Tokyo 173-8610, Japan.  
 Email: [okumura.yasuo@nihon-u.ac.jp](mailto:okumura.yasuo@nihon-u.ac.jp)

**Disclosures:** Yasuo Okumura belongs to the endowed departments of Boston Scientific Japan, Abbott Medical Japan, Japan Lifeline, Medtronic Japan, and Nihon Kohden.

## Funding information

Grant-in-Aid for Scientific Research (KAKENHI) from the Ministry of Education, Culture, Sports, Science and Technology of Japan, Grant/Award Number: 18K08117

## Abstract

**Background:** How obesity and epicardial fat influence atrial fibrillation (AF) is unknown.

**Methods:** To investigate the effect of obesity/epicardial fat on the AF substrate, we divided 20 beagle dogs of normal weight into four groups ( $n = 5$  each): one of the four groups (Obese-rapid atrial pacing [RAP] group) served as a novel canine model of obesity and AF. The other three groups comprised dogs fed a standard diet without RAP (Control group), dogs fed a high-fat diet without RAP (Obese group), or dogs fed a standard diet with RAP (RAP group). All underwent electrophysiology study, and hearts were excised for histopathologic and fibrosis-related gene expression analyses.

**Results:** Left atrial (LA) pressure was significantly higher in the Obese group than in the Control, RAP, and Obese-RAP groups ( $23.4 \pm 6.9$  vs.  $11.4 \pm 2.1$ ,  $11.9 \pm 6.4$ , and  $13.5 \pm 2.9$  mmHg;  $p = .005$ ). The effective refractory period of the inferior PV was significantly shorter in the RAP and Obese-RAP groups than in the Control group ( $p = .043$ ). Short-duration AF was induced at greatest frequency in the Obese-RAP and Obese groups ( $p < .05$ ). Epicardial fat/Fatty infiltration was greatest in the Obese-RAP group, and greater in the Obese and RAP groups than in the Control group. %interstitial fibrosis/fibrosis-related gene expression was significantly greater in the Obese-RAP and RAP groups ( $p < .05$ ).

**Conclusions:** Vulnerability to AF was associated with increased LA pressure and increased epicardial fat/fatty infiltration in our Obese group, and with increased epicardial fat/fibrofatty infiltration in the RAP and Obese-RAP groups. These may explain the role of obesity/epicardial fat in the pathogenesis of AF.

## KEYWORDS

atrial fibrillation, electrical properties, epicardial fat, fatty infiltration, highfat diet

## 1 | INTRODUCTION

Visceral adiposity, specifically, is associated with obesity/metabolic syndrome (MetS), and increased epicardial fat is an important reflection of such adiposity.<sup>1–3</sup> The systemic pro-inflammatory states related to obesity/MetS<sup>2,3</sup> and to epicardial fat itself have been linked to the pathogenesis of atrial fibrillation (AF).<sup>4–6</sup> In fact, numerous studies have shown an association between obesity/MetS and/or epicardial fat and both new-onset AF and progression of AF.<sup>5,7–9</sup> Nonetheless, the precise role played by obesity/epicardial fat in left atrial (LA) substrate remodeling and thereby in the progression of AF is not fully understood. In seeking to elucidate the mechanistic link, we investigated the electrophysiologic and structural properties of the LA and vulnerability to AF in a novel canine model of obesity and AF (induced by rapid atrial pacing [RAP]) against those in dogs subjected to one of three other experimental conditions that differed in terms of the presence versus absence of obesity and presence versus absence of RAP.

## 2 | METHODS

### 2.1 | Animals used and division of the animals into experimental groups

The experimental protocol was approved by the Institutional Animal Care and Use Committee of the Nihon University School of Medicine.

Twenty beagle dogs aged 3 years and of normal weight (8.4–13.7 kg) were used for the study. After 1 week of adaptive feeding, 10 of the dogs were provided a standard diet (300 g/day of adult dog food plus vitamin/mineral supplements [840 kcal/day]) for at least 20 weeks, and, to simulate obesity, the other 10 dogs were provided a high-fat diet (standard diet plus 235 g/day of white rice and 400 g/day of high-calorie dog food [2210 kcal/day]) for at least 20 weeks (median, 33 weeks). Five of the ten dogs fed a standard diet were not subjected to any further experimental manipulation (Control group), and the other five dogs underwent RAP for induction of AF (RAP group). RAP was performed continuously during the last 6 weeks of the dietary period. Five of the ten dogs fed a high-fat diet were not subjected to any further experimental manipulation (Obese group), and the other five dogs underwent RAP for induction of AF (Obese-RAP group). RAP was performed continuously in these five dogs (Obese-AF model dogs) during the last 6 weeks of the dietary period. The RAP procedure was as follows: a single pacemaker lead was placed at the right ventricular (RV) apex, and two leads were placed in the right atrium (RA): one at the right atrial appendage (RAA) and the other at the lateral wall. RAP was performed by delivery of double paces via the two leads. Pacing was performed in VVI mode from the RV apex at 40 bpm, and AV block was created by delivery of radiofrequency current from an ablation catheter that had been advanced through a short sheath placed in the femoral vein. Thereafter, two pacemakers were implanted in the

neck: one for pacing from the RV apex in VOO mode pacemaker Nuance SR RF PM1214 (St. Jude Medical Inc.) and at a pacing cycle length of 750 ms [80 bpm], and the other for RAP from Activia SC 37602 (Medtronic Inc.) (at a pacing cycle length of 177 ms [340 bpm]).

### 2.2 | Baseline study

Baseline characteristics of the individual dogs were assessed before electrophysiologic study (EPS) and histologic study, both of which were performed in all dogs. The assessment covered the body weight, body condition score (BCS), which is a quantitative and subjective method for evaluating body fat in dogs,<sup>10</sup> and hemodynamic status (i.e., systolic blood pressure [BP], diastolic BP, and left atrial [LA] pressure). The BCS evaluation is based on a visual assessment and palpation adopting a nine-point scale system, and four classes of BCS are classified: 1–3 = lean, 4 and 5 = ideal, 6 and 7 = overweight,  $\geq 8$  = obese dogs.<sup>10</sup> The systolic BP, diastolic BP, and LA pressure were each measured three times and averaged for the analysis. Values were then calculated for the four study groups.

### 2.3 | Intracardiac echocardiography

All dogs also underwent intracardiac echocardiography (ICE) by a phased-array 8 French, 4.5–11.5 MHz catheter (e.g., AcuNav Ultrasound Catheter, Biosense Webster Inc.) which works with the Vivid 7 system (GE Healthcare Technologies) before EPS. Two-dimensional (2D) long-axis ICE images were used to obtain the following measurements: width and length of the LA for calculation of the LA area, left ventricular (LV) ejection fraction, LV end-systolic and diastolic dimensions, and interventricular septum and posterior wall thicknesses. For the four group dogs, all recordings were obtained in sinus rhythm (SR).

### 2.4 | Preparation for EPS

In preparation for EPS, the dogs were anesthetized by intramuscular injection of 0.1 mg/kg midazolam, followed by inhalation of 2%–3% sevoflurane, and the anesthesia was maintained by continuous infusion of 7 mg/kg/h propofol. A tracheal cannula was inserted, and intermittent positive-pressure ventilation (tidal volume of 10 ml/kg, respiratory rate of 20 breaths/min) was applied by delivery of room air through a respirator. After deep anesthesia was established, vascular access was percutaneously achieved via the right external jugular vein and the right and left femoral veins and artery. Blood samples were then obtained, and plasma insulin, leptin, and von Willebrand factor levels and serum D-dimer concentrations were assessed between the four groups. Continuous surface electrocardiographic (ECG) and BP monitoring were begun. A 7F catheter was positioned in the distal coronary sinus (CS) for anatomic

guidance and to provide a reference for the timing of data acquisition. The ICE catheter was advanced to the level of the tricuspid annulus to measure the dimensions of each chamber and to guide transseptal catheterization.

## 2.5 | Electrophysiologic study

For EPS, transseptal catheterization was performed under fluoroscopic and ICE guidance. After transseptal puncture, an SL 0 long sheath (Abbott Inc.) was inserted into the LA. Upon termination of the burst RAP, spontaneous restoration of SR occurred in all RAP group and Obese-RAP group dogs. The 3D geometry of the RA, LA, and three pulmonary veins (PVs) was reconstructed with the use of EnSiteNavX 8.0 (Abbott Inc.). An eight-pole mapping catheter with 4-mm interelectrode spacing (Snake; Japan Lifeline Inc.) was used for mapping and the 3D reconstruction. A 3D activation map was created during acquisition of bipolar signals (filter setting, 30–500 Hz) from the mapping catheter. Electrograms recorded during SR were stored and analyzed off-line with the EnSiteNavX mapping system. Bipolar voltage amplitudes derived from three mapping points were averaged for each of eight LA/PV segments: the LA septum, the roof and posterior wall of the LA, the LA appendage (LAA), the CS, and the right and left superior PVs at the venoatrial junctions, and the common inferior PV ostium. Potentials with amplitudes > 0.5 mV were deemed normal-voltage potentials and coded in purple, and potentials < 0.2 mV were deemed low-voltage potentials and coded in red or gray.<sup>10</sup> The effective refractory period (ERP) (i.e., the longest premature coupling interval [S1–S2] that failed to result in atrial capture) was measured from the LA and from the venoatrial junctions (2 × threshold-current, 2-ms pulses) at basic cycle lengths of 400 ms with eight basic stimuli (S1), followed by a premature (S2) stimulus delivered in 10-ms decrements. ERPs were obtained at five different sites: the LAA, the posterior LA, the right and left superior PVs at their venoatrial junctions, and the common inferior PV ostium. At each site, the ERP was measured three times and averaged. AF was induced by 2-, 4-, 6-, 8-, and 10-s bursts of RAP (5 V) from the LAA, and the duration of AF (with AF defined as the arrhythmia lasting ≥ 1 s) was measured.

## 2.6 | Histologic examination of the dogs' hearts

After EPS, the animals were immediately euthanized with injection of KCL after experiment, and their hearts were removed, fixed in 10% formalin, and subjected to histologic analysis. Paraffin-embedded specimens were serially sectioned at 4- $\mu$ m thickness and stained with hematoxylin-eosin or Masson's Trichrome. Tissue from the LAA, the right and left venoatrial junctions, and the common inferior PV ostium was examined for fibrotic change, inflammatory change, and myocyte hypertrophy. The RA was not included in the analysis because of the potential effects of pacemaker lead implantation and AV node ablation. Masson's Trichrome-stained sections were used to evaluate interstitial fibrosis and fatty infiltration within the tissues, and

hematoxylin-eosin-stained sections were used to measure atrial myocytes. Images were acquired and digitized on the standard light microscope (Olympus, CX41; Olympus Corp.) with an attached digital camera (DP 27) and CellSens Entry software (Olympus Corp.). LA/PV tissues were examined at ×40 magnification for quantification of epicardial fat, fatty infiltration, and fibrotic changes and at ×400 magnification for measurement of myocytes size. Quantification was based on pixel counts and was facilitated by the use of software callipers in Adobe Photoshop (Adobe Systems Inc.). To quantify epicardial fat and fatty infiltration within the tissues, three sites on sections of LAA tissue and of tissue from the three venoatrial junctions were randomly selected, the extent of epicardial fat (which was defined by the adipose tissue located between the visceral pericardium [epicardium] and myocardium) was measured, and fatty infiltration was quantified as the ratio of the extent of fatty infiltration to wall thickness and reported as a percentage. Interstitial fibrosis was quantified as the ratio of the area of fibrotic myocardial tissue to that of normal myocardial tissue and reported as a percentage. Myocytes were measured at three randomly selected sites. Measurements were performed three times and averaged for the five individual animals in each group, and then mean group epicardial fat values, %fatty infiltration, %interstitial fibrosis, and myocyte size were determined.

## 2.7 | Gene expression analysis

Total RNA was extracted from the LA and venoatrial junction tissues with the use of TRIzol Reagent (Invitrogen; Thermo Fisher Scientific Inc.). Genomic DNA was removed from total RNA with use of gDNA Remover (Toyobo Co. Ltd.). Complementary DNA was synthesized from the resulting genomic DNA using ReverTra Ace qPCR RT Master Mix (Toyobo Co. Ltd.). All processes were performed according to the manufacturer's protocol. Fibronectin, collagen I, collagen III, and transforming growth factor (TGF)- $\beta$ 1 gene expression levels were assessed by quantitative polymerase chain reaction (qPCR) with the QuantStudio 3 Real-Time PCR System (Thermo Fisher Scientific Inc.) as follows: the mixtures were heated to 95°C for 30 s, followed by 45 cycles at 95°C for 3 s and 60°C for 30 s. The PCR primers used to amplify fibronectin, collagen I, collagen III, and TGF- $\beta$ 1 messenger RNA (mRNA) are shown in Table S1. Amplification of GAPDH served as an internal positive control and allowed normalization of the various mRNA levels against the total mRNA content in the samples.

## 2.8 | Statistical analysis

Continuous variables are shown as mean  $\pm$  SD or median and interquartile range, and categorical variables are shown as the percentage of animals per group. Between-group differences in study variables were subjected to one-way analysis of variance (one-way ANOVA) and Tukey post-hoc HSD test or to Kruskal–Wallis test and Wilcoxon post-hoc test. Mixed-effect models were fitted to the data to compare voltages, ERPs, and histologic findings (extent of epicardial fat, %fatty infiltration,

%interstitial fibrosis, and myocyte size) between the LA and venoatrial junction sites and between the study groups (Control, RAP, Obese, and Obese-RAP groups). Fixed effects of group, LA sites, and venoatrial junction sites were entered into the statistical model. Main effects and their interactions were tested. Animal IDs were entered as a random factor to account for nested data. Because epicardial fat, %fatty infiltration, %interstitial fibrosis were of skewed distribution, values were log-transformed for the mixed-effect models. If a significant interaction was found, post-hoc *p* values were obtained by Tukey HSD test. Relations between histologic findings and electrophysiologic variables (voltage and ERP) at the corresponding LA/PV sites was assessed on the basis of Spearman's correlation coefficient. All statistical analyses were performed with SAS 9.3 (SAS Institute Inc.), and *p* < .050 was considered statistically significant.

### 3 | RESULTS

#### 3.1 | Baseline body weight and hemodynamics, ICE measurements, and biomarker concentrations

Baseline body weight and hemodynamic variables, ICE measurements, and biomarker concentrations are shown per group in

Table 1. A high-fat diet significantly increased the body weight in the Obese and Obese-RAP groups (*p* < .05 vs. Control and RAP groups), resulting in significantly greater body weight and BCS in the Obese and Obese-RAP groups than in the Control and RAP groups (*p* < .001). Diastolic BP and LA pressure were significantly higher in the Obese group than in the Control, RAP, and Obese-RAP groups (*p* = .02 and *p* = .005, respectively). There was no between-group difference in systolic BP or ICE measurements. Insulin concentrations differed significantly between groups (*p* = .012), being significantly higher in the Obese group than in the Control and RAP groups and significantly higher in the Obese-RAP group than in the RAP group. There were no other between-group differences in biomarker levels.

#### 3.2 | EPS findings

LA conduction velocity, which was calculated on the basis of distance between the proximal electrodes and the distal CS electrodes, did not differ between the Control, RAP, Obese, and Obese-RAP groups (at  $0.81 \pm 0.14$  vs.  $0.68 \pm 0.08$  vs.  $0.68 \pm 0.11$  vs.  $0.68 \pm 0.08$  m/s, respectively; *p* = .16). A representative 3D voltage map is shown for each group in Figure 1A. There was no

**TABLE 1** Baseline body weight, hemodynamic variables, ICE measurements, and biomarker levels, per study group

	Control group	RAP group	Obese group	Obese-RAP group	<i>p</i> value
Body weight (kg)	11.7 ± 1.9	10.7 ± 1.4	18.2 ± 4.6*	17.6 ± 1.5*	<.001
Gained body weight (kg) by normal or high-fat diet	+2.6 ± 1.1	+1.1 ± 1.9	+7.1 ± 3.5*	+6.6 ± 1.5*	.001
Body condition score	5.2 ± 0.8	5.1 ± 1.5	8.1 ± 1.0*	7.5 ± 1.0*	<.001
Systolic BP (mmHg)	111.0 ± 18.8	114.0 ± 15.5	109.0 ± 14.3	125.6 ± 21.1	.47
Diastolic BP (mmHg)	65.8 ± 9.4	67.4 ± 11.5	88.2 ± 13.3*	73.2 ± 9.6	.02
LA pressure (mmHg)	11.4 ± 2.1	11.9 ± 6.4	23.4 ± 6.9**	13.5 ± 2.9	.005
ICE measurements					
LA area (cm <sup>2</sup> )	5.6 ± 1.3	3.8 ± 2.0	5.4 ± 1.3	5.7 ± 1.5	.23
IVSd (mm)	5.9 ± 0.5	7.0 ± 1.1	6.0 ± 1.7	7.2 ± 2.0	.36
PWd (mm)	6.8 ± 1.3	7.7 ± 1.0	7.2 ± 1.2	8.5 ± 0.6	.09
LVDd (mm)	25.7 ± 4.0	24.1 ± 5.8	26.2 ± 4.4	20.8 ± 4.4	.30
LVEF (%)	70.2 ± 5.6	63.6 ± 14.7	60.6 ± 6.1	69.6 ± 13.7	.46
Biomarker concentrations					
Insulin (mU/L)	6.9 (3.6–9.8)	5.7 (3.9–9.2)	14.4 (12.3–34.4)*	15.8 (9.1–55.4)***	.012
Leptin (ng/ml)	0.9 ± 0.4	0.7 ± 0.2	1.0 ± 0.2	0.8 ± 0.3	.35
vWF (%)	107 ± 38	80 ± 36	65 ± 38	88 ± 16	.30
D-Dimer (μg/ml)	0.27 (0.13–0.36)	0.35 (0.26–0.79)	0.25 (0.12–0.61)	0.48 (0.40–0.56)	.09

Note: Values are mean ± SD or median (interquartile range). *p* value by analysis of variance (ANOVA) or Kruskal–Wallis test.

Abbreviations: BP, blood pressure; ICE, intracardiac echocardiography; IVS, interventricular septal dimension at diastole; LA, left atrial; LVDd, left ventricular diastole dimension; LVEF, left ventricular ejection fraction; PW, posterior wall dimension at diastole; RAP, rapid atrial pacing; vWF, von Willebrand factor.

\**p* < .05 versus Control group and RAP groups; \*\**p* < .05 versus Control group, RAP group, and Obese-RAP group; \*\*\**p* < .05 versus RAP group by Tukey–Kramer post-hoc HSD test or Wilcoxon *t* test.

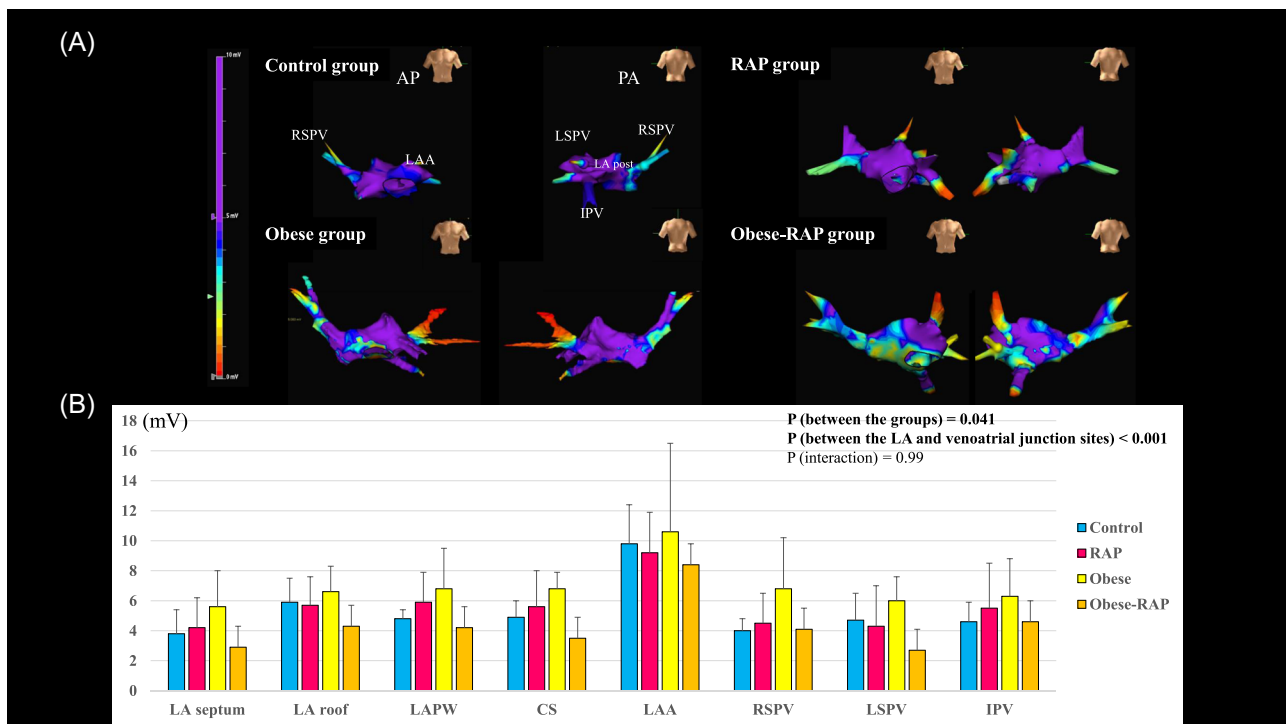


**FIGURE 1** Electrophysiology findings. (A) Representative 3D voltage maps of the LA and PVs. (B) Bar graph showing average bipolar voltage in each segment of the LA and venoatrial junction for the Control group, RAP group, Obese group, and Obese-RAP group. AP, anterior posterior view; CS, coronary sinus; IPV, venoatrial junction of the common inferior pulmonary vein; LA, left atrium; LAA, left atrial appendage; LAPW, LA posterior wall; LSPV, venoatrial junction of the left superior pulmonary vein; PV, pulmonary vein; RAP, rapid atrial pacing; RSPV, right superior pulmonary vein; PA, posterior anterior view

electrical impulse interference indicative of scarring in any region in any group, but bipolar voltage amplitudes from the five LA sites and three venoatrial junctions differed significantly between the four groups (Control,  $5.3 \pm 2.3$  mV; RAP,  $5.7 \pm 2.6$  mV; Obese,  $6.9 \pm 3.1$  mV; Obese-RAP,  $4.2 \pm 2.2$  mV;  $p = .041$ ) and between the LA and venoatrial junction sites ( $p < .001$ ) (Figure 1B). Global voltage amplitude was significantly lower in the Obese-RAP group than in the Obese group ( $p < .05$ ). The reduced voltage in the Obese-RAP group was consistent across the LA sites and the venoatrial junction sites (interaction  $p = .99$ ). Overall mean ERPs from the two LA and three venoatrial junction sites did not differ between groups ( $p = .28$ ), but the ERPs measured in the LA and at the venoatrial junctions differed between the groups (interaction  $p = .020$ ). This was due to a significantly shorter ERP in the common inferior PV in the RAP and Obese-RAP groups ( $121.0 \pm 47.2$  and  $122.0 \pm 37.0$  ms, respectively) than in the Control group ( $182.0 \pm 31.1$  ms) ( $p = .043$ ) (Figure 2A). Burst pacing-induced AF was significantly more prevalent in the Obese and Obese-RAP groups than in the RAP and Control groups (63% and 68%, respectively, vs. 32% and 16%, respectively;  $p < .001$ ). The AF lasted longer in the Obese-RAP and Obese groups than in the RAP and Control groups (Obese-RAP, 3 [0–5.5] s; Obese, 2 [0.5–2.8] s; RAP, 0 [0–4.5] s; Control, 0 [0–0] s;  $p < .001$ ) (Figure 2B).

### 3.3 | Results of histopathologic analysis

Representative histopathology slides from the four groups are shown in Figures 3 and 4. In the Control group, a few adipocytes were seen in the epicardium, whereas in the RAP, Obese, and Obese-RAP groups, abundant adipose tissue was seen in the epicardium, and fatty infiltration of the atrial tissues was evident (Figure 3A). The extent of epicardial fat and %fatty infiltration in the LAA and at the three venoatrial junction sites differed significantly between the four groups (extent of epicardial fat: Control, 93 [41–179]  $\mu$ m; RAP, 249 [178–355]  $\mu$ m; Obese, 233 [136–329]  $\mu$ m; Obese-RAP, 334 [243–550]  $\mu$ m;  $p = .006$ ; %fatty infiltration: Control, 7.3 [0.7–17.1] %; RAP, 29.3 [21.4–47.6] %; Obese, 27.9 [12.5–31.7] %; Obese-RAP, 43.1 [38.6–48.6] %;  $p < .001$ ). In particular, the extent of epicardial fat was significantly greater in the RAP, Obese, and Obese-RAP groups than in the Control group ( $p < .05$  for RAP, Obese, and Obese-RAP groups vs. Control group) (Figure 3B). The %fatty infiltration was also significantly greater in RAP, Obese, and Obese-RAP groups than in Control groups ( $p < .05$  for RAP, Obese, and Obese-RAP groups vs. Control group;  $p < .05$  for RAP and Obese groups vs. Obese-RAP group) (Figure 3C). The % interstitial fibrosis at the LAA and three venoatrial junction sites also differed between the four groups (Control 1.5 [0.6–1.9] %; RAP 5.1 [2.4–6.7] %;

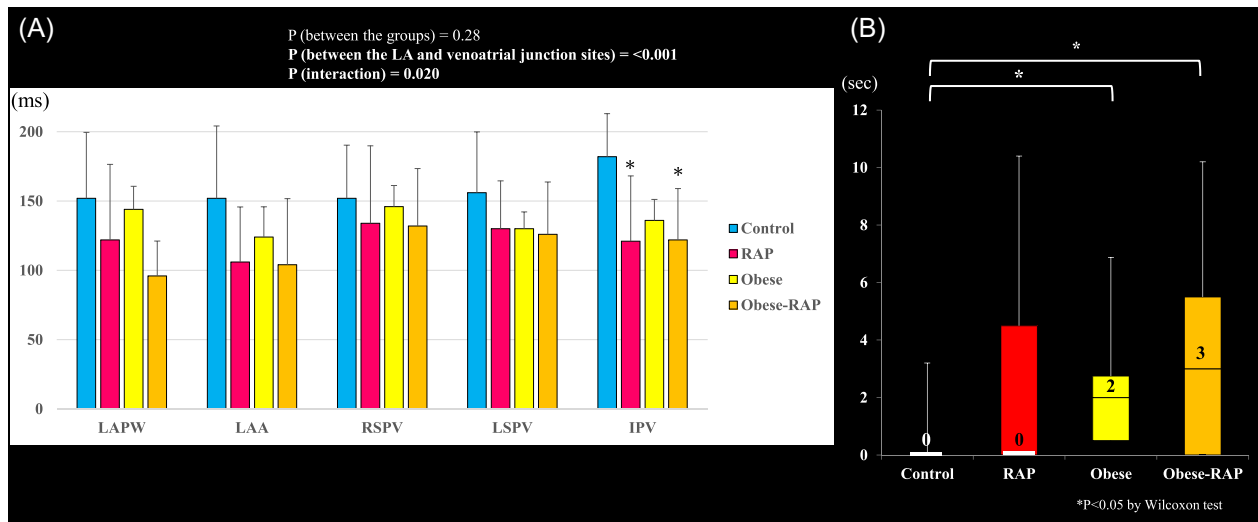


**FIGURE 2** Further electrophysiology findings. (A) Effective refractory periods in each segment of the LA and venoatrial junctions, per study group, and (B) duration of AF induced by rapid atrial pacing, per study group. AF, atrial fibrillation; other abbreviations are as in Figure 1

Obese 1.4 [0.8–2.6] %; Obese-RAP 4.1 [2.8–6.2] %,  $p = .002$ ), with %interstitial fibrosis being significantly greater in the Obese-AF and RAP groups than in the other two groups ( $p < .05$  for Control and Obese groups vs. RAP and Obese-RAP groups) (Figure 3D,E). The size of atrial myocytes at the LAA and the three venoatrial junction sites also differed between the groups (Control  $12.4 \pm 0.1 \mu\text{m}$ ; RAP  $17.6 \pm 2.4 \mu\text{m}$ ; Obese  $16.8 \pm 2.8 \mu\text{m}$ ; Obese-RAP  $17.1 \pm 2.3 \mu\text{m}$ , respectively;  $p < .001$ ), with the atrial myocytes being significantly larger in the RAP, Obese, and Obese-RAP groups than in the Control group ( $p < .05$ ) (Figure 3F,G).

The extent of epicardial fat and %fatty infiltration correlated modestly with %interstitial fibrosis at the corresponding LA/PV sites ( $r = .39$ ,  $p = .001$ ;  $r = .40$ ,  $p < .001$ , respectively) (Figure 4A). No correlation was found between epicardial fat extent/%fatty infiltration and voltages and ERP at the corresponding LA/PV sites (Figure 4B, C). Correlation was also not found between % interstitial fibrosis and voltage, but significant correlation was found between %interstitial fibrosis and ERP ( $r = -0.33$ ;  $p = .004$ ) (Figure 4D).

### 3.4 | Gene expression

Between-group differences were found in the fibronectin, collagen I, collagen III, and TGF- $\beta$ 1 mRNA expression levels ( $p < .05$  for all) (Figure 5). Fibronectin, collagen I, collagen III, and TGF- $\beta$ 1 mRNA expression levels were significantly increased in the Obese-RAP group compared to levels in the Control group ( $p < .05$ ). The fibronectin 1 mRNA expression level in the Obese-RAP group was significantly greater than that in the Obese group ( $p < .05$ ), and the collagen III mRNA expression level in the Obese-RAP and RAP groups was significantly greater than that in the Obese group ( $p < .05$ ).

## 4 | DISCUSSION

This study revealed mechanistic details of atrial remodeling promoted by RAP-induced AF alone, obesity alone, and obesity with RAP-induced AF. Bipolar voltage amplitudes within the LA and at the venoatrial junctions were highest in the Obese group and lowest in the Obese-RAP group. Globally, ERPs of the LA and venoatrial junctions did not differ, but the common inferior PV ERP was significantly shorter in the RAP and Obese-RAP groups than in the other two groups. Duration of AF induced by burst pacing was slightly longer in the Obese-RAP and Obese groups than in the other two groups. The extent of epicardial fat and % fatty infiltration were greatest in the Obese-RAP group, and these two variables tended to be increased in the RAP and Obese groups. The %interstitial fibrosis was significantly greater in the Obese-RAP and RAP groups than in the Obese and Control groups. Expression levels of fibronectin 1, collagen I, collagen III, and TGF- $\beta$ 1 mRNA were upregulated in the Obese-RAP group and RAP group in comparison to levels in the other two groups.

### 4.1 | Effect of obesity and RAP-induced AF on atrial hemodynamic, electrical, and structural properties

In this study, a sustained high-fat diet during a median of 33-week successfully created obese dogs, as represented by a significantly higher body weight and BCS in the Obese and Obese-RAP models than in the Control and RAP models. In particular, the Obese-RAP model is a novel canine model of obesity and AF by means of RAP. Regarding the electrical properties, the ERP in the common inferior PV was significantly decreased only in the Obese-RAP and RAP group dogs. Wiffel used RAP to create

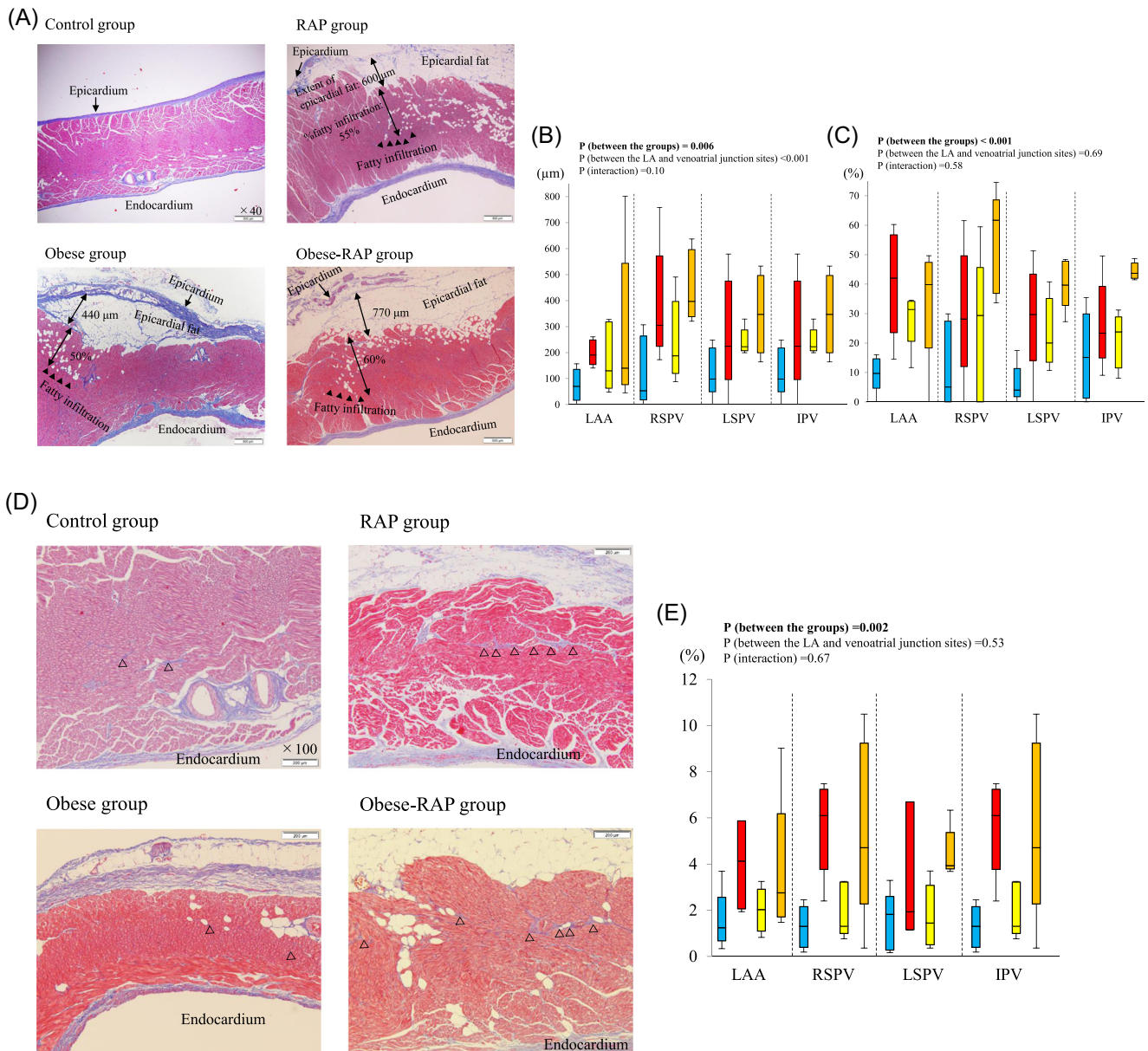


**FIGURE 3** Histopathologic findings in each of the four study groups. (A) Representative Masson's staining of the sections of the venoatrial junction of pulmonary vein for evaluation of the extent of epicardial fat (adipose tissue located between the epicardium and myocardium) and %fatty infiltration (▲). (B) Bar graph showing the extent of epicardial fat in each segment of the LA and at the venoatrial junctions. (C) Bar graph showing %fatty infiltration. (D) Representative Masson's staining of the sections of the venoatrial junction tissues showing the interstitial fibrosis (△). (E) Bar graph showing %interstitial fibrosis. (F) Representative hematoxylin-eosin staining of venoatrial junction tissues for evaluation of the size of myocytes (magnified images). (G) Bar graph showing myocyte size in each segment of the LA and at the venoatrial junctions. Values in panel A indicate the extent of epicardial fat and %fatty infiltration. Abbreviations are as in Figure 1

a swine model of AF and found the electrophysiologic properties relevant to the development and maintenance of AF to be a shortened atrial ERP and prolonged atrial conduction time.<sup>11</sup> Such so-called “electrical remodeling” has been reported to represent the early stage of AF progression.<sup>11,12</sup> Our results point to the presence of electrical remodeling that promotes susceptibility to AF in the Obese-RAP group, with similar susceptibility promoted in the RAP group.

We found that voltages were lowest in Obese-RAP group despite no apparent low-voltage area in any of the four groups. Further, a modest interstitial fibrotic change in the LA supported by the increased expression of collagen-related fibronectin 1, collagen I, collagen III, and TGF-β1 genes<sup>13,14</sup> was observed in the Obese-RAP and RAP groups. Perpetual AF causes atrial electrical remodeling in the early stage, leading to structural remodeling, which is accompanied by a progressive increase in atrial interstitial fibrosis,



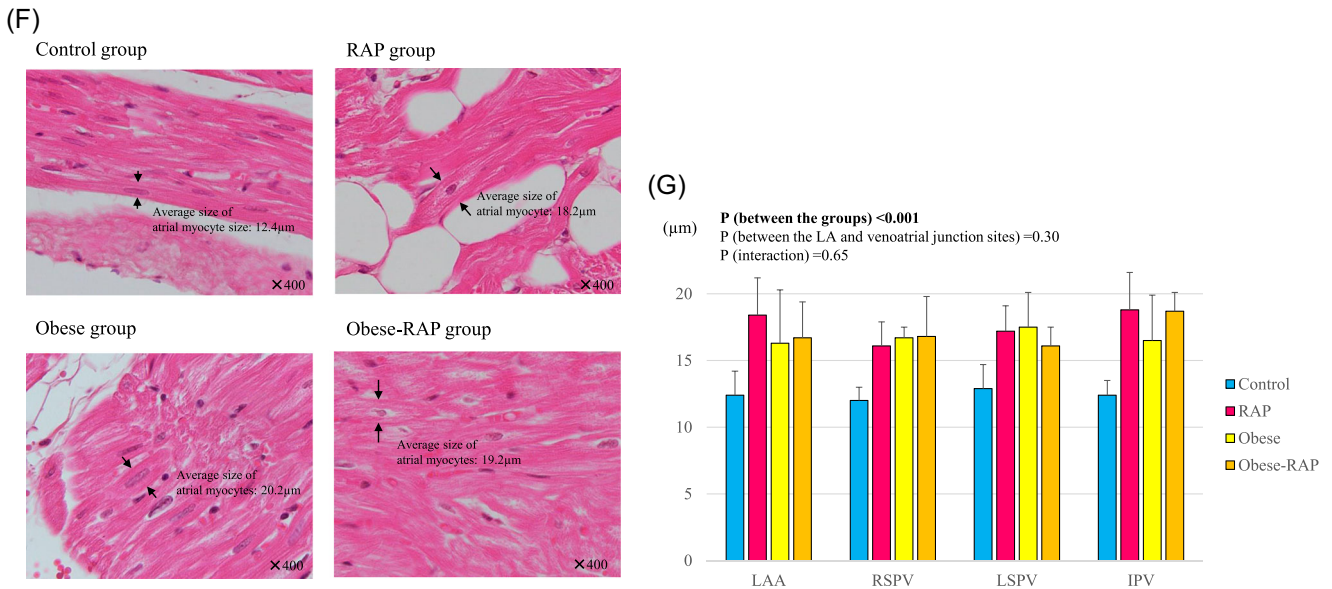


**FIGURE 3** Continued

hypertrophy, and/or dilatation.<sup>11</sup> Therefore, those data indicate that the RAP-induced AF produced interstitial fibrosis. Regarding the AF inducibility, AF was most frequently induced in the Obese-RAP group than in the other groups, and the duration of AF was greatest in this group. Short-duration AF was also induced frequently in our Obese group. There would be several mechanistic factors promoting AF substrates by obesity including inflammation,<sup>2,3,15</sup> autonomic disturbances,<sup>16,17</sup> and atrial stretch due to increased atrial pressure.<sup>18–21</sup> Although the Obese and Obese-RAP models

potentially had insulin resistance (as reflected by elevated insulin levels), this study did not have any apparent observations supporting inflammation or an autonomic disturbance produced by obesity. Nonetheless, the systemic diastolic BP and LA pressure were significantly increased in the Obese group, and marginally more increased in the Obese-RAP group than in the RAP and Control groups. These underlying conditions might have produced atrial and PV stretch. Acute atrial stretch reduces the atrial ERP and depresses atrial conduction velocity, potentially through a reduction in cellular

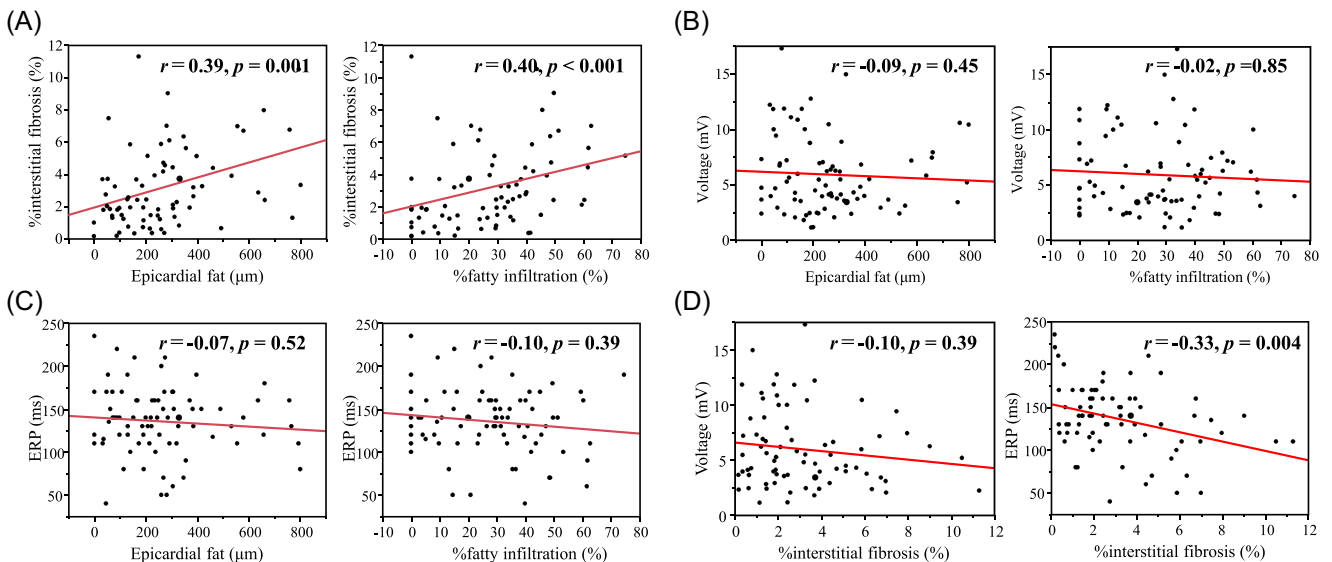


**FIGURE 4** Scatter plots showing correlation (A) between the extent of epicardial fat and %fatty infiltration and extent of epicardial fat and %interstitial fibrosis and (B) between the extent of epicardial fat and %fatty infiltration and extent of epicardial fat and voltage, and (C) between the extent of epicardial fat and fatty infiltration extent of epicardial fat and ERP and (D) between %interstitial fibrosis and voltage and % interstitial fibrosis and ERP

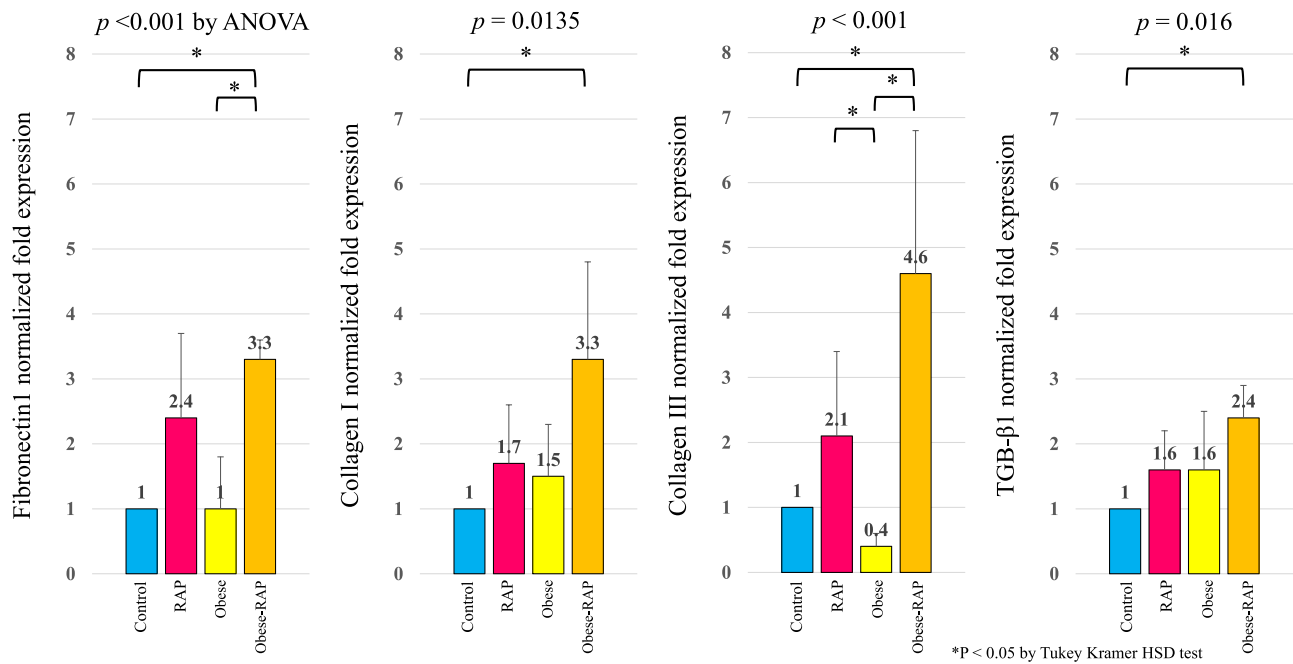


**FIGURE 5** Bar graphs showing results of real-time RT-PCR analysis of fibronectin 1, collagen I, collagen III, and TGF-β1 mRNA expression levels in LA and venoatrial junction tissues in the four study groups. Abbreviations are as in Figure 1

excitability by the opening of stretch-activated channels.<sup>19,20</sup> In an optical mapping study conducted by Kalifa et al.<sup>21</sup> AF was induced by gradual increases in atrial pressure. In a clinical study regarding the electrophysiologic characteristics conferred by obesity,<sup>18</sup> the ERPs in the PV were substantially shorter in patients with a normal body mass index (BMI) than in those with an increased BMI. These hemodynamic conditions may lead to atrial hypertrophy,<sup>22,23</sup> which might explain the highest bipolar voltage reflecting hypertrophied myocytes seen in our Obese group. Both the RAP and Obese-RAP dogs also had hypertrophied myocytes but the high bipolar voltages were not observed. This is due possibly to the fact that the fibrotic change in these two groups might have lessened the increase in bipolar voltages from hypertrophied myocytes. Taken together, our findings suggest that obesity alone promotes vulnerability to AF by electrical remodeling due to an increased LA pressure. Further, the greater histological changes and gene expression in the Obese-RAP group than in the RAP group implicated that obesity may foster vulnerability to AF and interstitial fibrosis via a modest increased LA pressure. In the clinical situation, the Obese group characteristics may be representative of early-stage AF remodeling in obese patients, while the Obese-RAP group characteristics represent that structural remodeling may be augmented once AF is maintained under an obese condition.

#### 4.2 | Effect of epicardial fat on atrial remodeling

We found significant fatty infiltration and epicardial fat in the RAP, Obese, and Obese-RAP groups. Our canine model of Obese and AF

indicated that both epicardial fat and fatty infiltration are produced not only by obesity but also by sustained AF. Multiple mechanisms by which epicardial fat leads to AF have been considered: (1) activation of the pro-inflammatory cytokines released from the epicardial fat, leading to fibrosis of the neighboring atrial myocardium; (2) direct infiltration of adipocytes contained in the abundant epicardial fat into the underlying atrial tissue; (3) firing of ganglionated plexi in the epicardial fat; and (4) compression due to the increased epicardial fat around the heart, leading to restrictive LV diastolic filling and subsequent atrial dilation.<sup>24</sup>

Among the total 20 animals in our study, epicardial fat and % fatty infiltration correlated modestly with %interstitial fibrosis, suggesting that fatty deposits in the tissues produces fibrosis. Nonetheless, significant fibrotic change and upregulated collagen-related mRNAs were observed in the RAP and Obese-RAP groups but not in the Obese group. In contrast, in an ovine model of obesity, produced by feeding the animals a high-fat diet for 1 year, significant fatty infiltration and fibrotic change matched those seen in sheep fed a normal diet.<sup>25</sup> Therefore, fibrotic change due simply to obesity might require longer-term administration of a high-fat diet. Studies have indicated that fatty infiltration itself may contribute to the maintenance of AF. For example, fatty infiltration itself may be the underlying factor characterizing the substrate of conduction heterogeneity during AF.<sup>25</sup> In a human study, the locations or volume of epicardial fat correlated well with electrically fractionated potentials recorded during AF.<sup>15,26</sup> We did not find any direct association between fatty infiltration and electrical variables such as ERPs and voltages. Rather, %interstitial fibrosis correlated modestly with a shortened ERP, which can be the substrate for conduction

heterogeneity. Therefore, neither epicardial fat nor fatty infiltration may be the culprit factor in vulnerability to AF. Rather, each might act as a promotor for fibrotic change, which serves as a critical substrate for AF. The role of epicardial fat and fatty infiltration in the pathogenesis of AF may be multifactorial. Thus, further studies are needed to clarify this point.

## 5 | LIMITATIONS

Our findings must be considered in light of our study limitations, the first of which is its size. Only a small number of animals were included in each group, and this might have led to the absence of statistically significant differences in several crucial variables. Second, the optimal duration to create obesity/MetS in beagle dogs has not been fully established yet. The 33-week-exposure to a high-fat diet in 3-year-old beagle dogs would be sufficient to induce obesity because the body weight (17–18 kg) and BCS (7–8) in our obese models was as high as or rather higher than that in an obese model reported previously.<sup>10</sup> Finally, because of the difficulty in obtaining male adult dogs for research in Japan, we only included female beagles. It has been reported that the female sex is associated with overweight/obese dogs,<sup>27</sup> so female sex may affect the increased body weight in our obese model.

## 6 | CONCLUSIONS

Vulnerability to AF was associated with increased LA pressure, increased epicardial fat, and fatty infiltration in the heart in our Obese group, and with increased epicardial fat and fibrofatty infiltration in the RAP and Obese-RAP groups. These observations provide mechanistic insight into the role played by obesity, and epicardial fat in particular, in the pathogenesis of AF.

### ACKNOWLEDGMENTS

The author thanks Ms Wendy Alexander-Adams and Mr John Martin for their encouragement and assistance in the preparation of this commentary in English.

### FUNDING INFORMATION

This study was supported in part by a Grant-in-Aid for Scientific Research (KAKENHI) from the Ministry of Education, Culture, Sports, Science and Technology of Japan (18K08117).

### ORCID

Naoto Otsuka  <http://orcid.org/0000-0002-6931-8522>

Yasuo Okumura  <https://orcid.org/0000-0002-2960-4241>

Koichi Nagashima  <http://orcid.org/0000-0003-2326-225X>

Yuji Wakamatsu  <http://orcid.org/0000-0002-1540-8514>

Seina Yagyu  <http://orcid.org/0000-0002-6115-1860>

Toshiko Nakai  <http://orcid.org/0000-0002-7346-6085>

## REFERENCES

- Rosito GA, Massaro JM, Hoffmann U, et al. Pericardial fat, visceral abdominal fat, cardiovascular disease risk factors, and vascular calcification in a community-based sample: the Framingham Heart Study. *Circulation*. 2008;117:605-613.
- Ridker PM, Buring JE, Cook NR, Rifai N. C-reactive protein, the metabolic syndrome, and risk of incident cardiovascular events: an 8-year follow-up of 14719 initially healthy American women. *Circulation*. 2003;107:391-397.
- Cho DH, Joo HJ, Kim MN, Lim DS, Shim WJ, Park SM. Association between epicardial adipose tissue, high-sensitivity C-reactive protein and myocardial dysfunction in middle-aged men with suspected metabolic syndrome. *Cardiovasc Diabetol*. 2018;17:95.
- Monno K, Okumura Y, Saito Y, et al. Effect of epicardial fat and metabolic syndrome on reverse atrial remodeling after ablation for atrial fibrillation. *J Arrhythm*. 2018;34:607-616.
- Nagashima K, Okumura Y, Watanabe I, et al. Association between epicardial adipose tissue volumes on 3-dimensional reconstructed CT images and recurrence of atrial fibrillation after catheter ablation. *Circ J*. 2011;75:2559-2565.
- Chung MK, Martin DO, Sprecher D, et al. C-reactive protein elevation in patients with atrial arrhythmias: inflammatory mechanisms and persistence of atrial fibrillation. *Circulation*. 2001;104:2886-2891.
- Benjamin EJ, Levy D, Vaziri SM, D'Agostino RB, Belanger AJ, Wolf PA. Independent risk factors for atrial fibrillation in a population-based cohort. The Framingham Heart Study. *JAMA*. 1994;271:840-844.
- Wang TJ, Parise H, Levy D, et al. Obesity and the risk of new-onset atrial fibrillation. *JAMA*. 2004;292:2471-2477.
- Watanabe H, Tanabe N, Watanabe T, et al. Metabolic syndrome and risk of development of atrial fibrillation: the Niigata preventive medicine study. *Circulation*. 2008;117:1255-1260.
- Liu DJX, Stock E, Broeckx BJG, et al. Weight-gain induced changes in renal perfusion assessed by contrast-enhanced ultrasound precede increases in urinary protein excretion suggestive of glomerular and tubular injury and normalize after weight-loss in dogs. *PLoS One*. 2020;15:e0231662.
- Wijffels MC, Kirchhof CJ, Dorland R, Allessie MA. Atrial fibrillation begets atrial fibrillation. A study in awake chronically instrumented goats. *Circulation*. 1995;92:1954-1968.
- Allessie M, Ausma J, Schotten U. Electrical, contractile and structural remodeling during atrial fibrillation. *Cardiovasc Res*. 2002;54:230-246.
- Lijnen PJ, Petrov VV, Fagard RH. Induction of cardiac fibrosis by transforming growth factor-beta(1). *Mol Genet Metab*. 2000;71:418-435.
- Boldt A, Wetzel U, Lauschke J, et al. Fibrosis in left atrial tissue of patients with atrial fibrillation with and without underlying mitral valve disease. *Heart*. 2004;90:400-405.
- Mahajan R, Nelson A, Pathak RK, et al. Electroanatomical remodeling of the atria in obesity: impact of adjacent epicardial fat. *JACC Clin Electrophysiol*. 2018;4:1529-1540.
- Guarino D, Nannipieri M, Iervasi G, Taddei S, Bruno RM. The role of autonomic nervous system in pathophysiology of obesity. *Front Physiol*. 2017;8:665.
- Iso K, Okumura Y, Watanabe I, et al. Is vagal response during left atrial ganglionated plexi stimulation a normal phenomenon? comparison between patients with and without atrial fibrillation. *Circ Arrhythm Electrophysiol*. 2019;12:e007281.
- Munger TM, Dong YX, Masaki M, et al. Electrophysiological and hemodynamic characteristics associated with obesity in patients with atrial fibrillation. *J Am Coll Cardiol*. 2012;60:851-860.

19. Ravelli F, Allessie M. Effects of atrial dilatation on refractory period and vulnerability to atrial fibrillation in the isolated Langendorff-perfused rabbit heart. *Circulation*. 1997;96:1686-1695.
20. Bode F, Katchman A, Woosley RL, Franz MR. Gadolinium decreases stretch-induced vulnerability to atrial fibrillation. *Circulation*. 2000;101:2200-2205.
21. Kalifa J, Jalife J, Zaitsev AV, et al. Intra-atrial pressure increases rate and organization of waves emanating from the superior pulmonary veins during atrial fibrillation. *Circulation*. 2003;108:668-671.
22. Kume O, Takahashi N, Wakisaka O, et al. Pioglitazone attenuates inflammatory atrial fibrosis and vulnerability to atrial fibrillation induced by pressure overload in rats. *Heart Rhythm*. 2011;8:278-285.
23. De Jong AM, Van Gelder IC, Vreeswijk-Baudoin I, Cannon MV, Van Gilst WH, Maass AH. Atrial remodeling is directly related to end-diastolic left ventricular pressure in a mouse model of ventricular pressure overload. *PLoS One*. 2013;8:e72651.
24. Hatem SN, Redheuil A, Gandjbakhch E. Cardiac adipose tissue and atrial fibrillation: the perils of adiposity. *Cardiovasc Res*. 2014;102:205-213.
25. Mahajan R, Lau DH, Brooks AG, et al. Electrophysiological, Electroanatomical, and Structural Remodeling of the Atria as Consequences of Sustained Obesity. *J Am Coll Cardiol*. 2015;66:1-11.
26. Nagashima K, Okumura Y, Watanabe I, et al. Does location of epicardial adipose tissue correspond to endocardial high dominant frequency or complex fractionated atrial electrogram sites during atrial fibrillation? *Circ Arrhythm Electrophysiol*. 2012;5:676-683.
27. Usui S, Yasuda H, Koketsu Y. Characteristics of obese or overweight dogs visiting private Japanese veterinary clinics. *Asian Pac J Trop Biomed*. 2016;6:338-343.

#### SUPPORTING INFORMATION

Additional Supporting Information may be found online in the supporting information tab for this article.

**How to cite this article:** Otsuka N, Okumura Y, Arai M, et al. Effect of obesity and epicardial fat/fatty infiltration on electrical and structural remodeling associated with atrial fibrillation in a novel canine model of obesity and atrial fibrillation: A comparative study. *J Cardiovasc Electrophysiol*. 2021;32:889-899. <https://doi.org/10.1111/jce.14955>

# 心房細動の電氣的、構造的リモデリングにおける肥満と心外膜脂肪の影響 —肥満心房細動イヌモデルによる検討—

## 抄録

### 【背景】

糖尿病、高血圧、肥満を含んだメタボリック症候群は、全身の炎症の惹起を通して心房細動 (Atrial Fibrillation: AF) の進行に寄与する。また、メタボリック症候群の表現型である心外膜脂肪と心房筋の電氣的、構造的リモデリングに密接な関連があることは報告されている。しかしながら、肥満と心外膜脂肪が心房細動リモデリングに寄与する機序は十分に解明されていない。本研究では、われわれが開発した肥満AFイヌモデルにより、肥満および心外膜脂肪のAF進展に寄与する機序を明らかにすることを目的とした。

### 【方法】

ビーグル犬 20 頭を対象に、24 週間高カロリー食を給与し、後半の 4~8 週間は高頻度心房刺激 (Rapid atrial pacing: RAP) を行い臨床的な AF を模擬した肥満合併 RAP 群 (Obese-RAP 群: 5 頭)、通常食に同様の RAP を行う群 (RAP 群: 5 頭)、高脂肪食のみを与える肥満群 (Obese 群: 5 頭)、通常食のみを与える対照群 (Control 群: 5 頭) に分け、電気生理学的検査、組織学的、分子生物学的検証を行った。

### 【結果】

体重は、Obese-RAP 群、Obese 群でそれぞれ  $17.6 \pm 1.5\text{kg}$ 、 $18.2 \pm 4.6\text{kg}$  であり、Control 群  $11.7 \pm 1.9\text{kg}$ 、RAP 群  $10.7 \pm 1.4\text{kg}$  より高値を呈し、肥満イヌモデルの作成に成功した。左房圧は、Control 群  $11.4 \pm 2.1\text{mmHg}$ 、RAP 群  $11.9 \pm 6.4\text{mmHg}$ 、Obese-RAP 群  $13.5 \pm 2.9\text{mmHg}$ 、Obese 群  $23.4 \pm 6.9\text{mmHg}$  であり、Obese 群が有意に上昇していた。電気生理学的検査 (Electrophysiologic study: EPS) では、Control 群や Obese 群と比較して RAP 群が、心房筋の障害を反映する左房・肺静脈の有効不応期 (Effective refractory period: ERP) が短く、Obese-RAP 群ではさらに短縮していた。高頻度連続刺激による AF 持続時間は、Control 群 0(0-1)秒、RAP 群 0(0-4.5)秒、Obese 群 2(0-3.5)秒、Obese-RAP 群 3(0-3.5)秒と段階的に延長した。組織学的には、心外膜脂肪が Control 群、RAP 群、Obese 群、Obese-RAP 群で段階的に増加し、心房筋への脂肪浸潤も同様の傾向を認めた。線維化の程度も 4 群間で有意差を認め、RAP 群、Obese-RAP 群は他の 2 群と比較して大きかった。また、組織学的な心外膜脂肪の厚さおよび心房筋への脂肪浸潤の程度が、線維化の程度と中等度の相関がみられた (心外膜脂肪:  $r=0.39$ 、心房筋への脂肪浸潤:  $r=0.40$ )。心外膜脂肪の厚さおよび心房筋への脂肪浸潤の程度は左房・肺静脈不応期の短縮とは相関がみられなかったが、線維化の程度は不応期の短縮と有意に相関していた ( $r=-0.33$ )。分子生物学的検証では、

線維化関連マーカーである I 型、III 型コラーゲン、TGF- $\beta$ 1 の mRNA の発現は、Control 群、Obese 群よりも RAP 群、Obese-RAP 群で増加しており、特に Obese-RAP 群では Control 群より有意であった ( $P < 0.05$ )。

#### 【考察】

本研究から、心外膜脂肪の厚さおよび心房筋への脂肪浸潤は、肥満単独のみならず AF 単独の存在でも生じ、さらに肥満に AF が合併すると心外膜脂肪や脂肪浸潤の程度がさらに促進されることが明らかになった。組織学的線維化は、24 週間の肥満単独の Obese 群では認めず、RAP 群、Obese-RAP 群で認め、分子生物学的検証においても線維化関連マーカーは同様の傾向を呈していた。組織学的、分子生物学的に線維化が亢進していた RAP 群、Obese-RAP 群では左房・肺静脈の ERP 短縮がみられ、Obese-RAP 群が最も短縮していた。また、全体解析においても、不応期の短縮と線維化の程度との相関がみられた。以上から、従来の報告と同様に線維化の存在が心房筋の不応期を規定する主因であり、Obese-RAP 群における構造的リモデリングが最も進展していることが示唆された。本研究では、心外膜脂肪、心房筋への脂肪浸潤の程度が線維化の程度との相関を認めたことが新知見であり、これは、心外膜脂肪や脂肪浸潤は線維化を促進する律速因子である可能性を支持する重要な所見であると言える。一方、Obese 群では、高頻度刺激による AF 持続時間が Control 群や RAP 群より延長しており、僅かな AF の器質を有していると言える。組織学的な心外膜脂肪の厚さおよび心房筋への脂肪浸潤が AF 器質を規定している可能性もあるが、ERP 短縮は RAP 群や Obese-RAP 群ほど見られていなかったことから、血行動態的な左房圧の上昇が関連していたのかもしれない。

#### 【結語】

本研究では、肥満単独の Obese 群において AF 器質を軽度有しており、これは左房圧の上昇や心外膜脂肪/脂肪浸潤の増加が関連していることが示唆された。一方、AF 単独の RAP 群および肥満合併 AF モデルである Obese-RAP 群では、組織学的に心外膜脂肪、脂肪浸潤、線維化の進展が見られ、特に Obese-RAP 群では電気生理学的、構造的リモデリングが進行していた。本研究から、肥満、AF 両者は AF 進展を亢進させ、心外膜脂肪や脂肪浸潤は AF 器質の主体である線維化を促進する律速因子である可能性が示唆された。

## 学位論文(日本語要約)

### 【緒言】

糖尿病、高血圧、肥満を含んだメタボリック症候群は、全身の炎症の惹起を通して心房細動 (AF) の進行に寄与する<sup>①</sup>。また、メタボリック症候群の表現型である心外膜脂肪 (Epicardial Fat: EAT) は、心房筋の電氣的、構造的リモデリングと密接な関連性が示唆されており、実際に EAT と AF 発生および進行と関連性があることが多くの臨床研究で報告されている<sup>2-4</sup>。以前にも我々は、ヒトでの EAT 量が AF 器質に影響を与えることを報告しており<sup>2</sup>、EAT と心房細動についての研究を行っている。EAT が AF を引き起こす機序として、以下の3つの機序が推察されている。第一として EAT から放出される炎症性サイトカインである。EAT から TNF $\alpha$ 、IL-6 などの炎症性サイトカインが分泌され、EAT が隣接する心房筋に影響を及ぼし線維化を引き起こす。特に、EAT に多く存在する Activin A の存在により、局所の心房筋線維化に関与していることが報告されている。第二に、EAT 内に存在する Ganglionated Plexus (GP) と呼ばれる心臓周囲の自律神経叢の役割である。GP からの異常興奮が、肺静脈からの心房期外収縮を発生させ、AF 発症維持を促進させる<sup>⑤</sup>。第三に、心臓周辺の EAT 増加による心房壁や左室壁への直接圧迫が、心房、心室の拡張を制限するため、左房圧の上昇を来し AF 器質を形成する<sup>⑥</sup>。これらの機序が推察されているが、未知な部分も多く、これらの因子がどの程度関連しているかは明らかではない。また、肥満や EAT の心房筋への直接的な影響を電気生理学的、組織学的両側面から、実験的に証明した報告は少ない。今までにヤギを用いた 2-4 週間の rapid pacing モデルやヒツジを用いた肥満モデルでの実験は行われているが、高脂肪食を投与した肥満イヌモデルに、より長期の心房細動を模した rapid pacing を行った、世界初の肥満 AF イヌモデルを使用した。そこで本研究では、我々が開発した世界初の肥満 AF イヌモデルを用い、肥満およびその表現型である EAT の AF 進展に寄与する機序を実験的に証明することを目的とした。

### 【方法】

本研究は、日本大学医学部内での倫理委員会の承認を受けた。

20 頭のビーグル犬を対象に、24 週間高カロリー食を給与し、後半の 6 週間は高頻度心房刺激 (rapid atrial pacing: RAP) を行い臨床的な AF を模擬した肥満合併 RAP 群 (Obese-RAP 群: 5 頭)、通常食に同様の高頻度心房刺激を行う群 (RAP 群: 5 頭)、高脂肪食のみを与える肥満群 (Obese 群: 5 頭)、通常食のみを与える対照群 (Control 群: 5 頭) に分割した。RAP 群、Obese-RAP 群の RAP モデルは、2 本のペースメーカーリードを右心耳と側壁に、1 本のペースメーカーリードを右室心尖部に留置し、房室ブロックを作成後、心房刺激を 340 回/分で、心室刺激を 80 回/分で設定した。全例、以下の手順で、電気生理学的検査、

組織学的、分子生物学的検証を行った。

- ・体重、体格評価

電気生理学的検査前に、体重測定を行い、犬の肥満度は body condition score (BCS) score を使用し、視覚的評価を行った<sup>7</sup>。

- ・心腔内超音波

電気生理学的検査前に心腔内超音波を用い、洞調律中の左房径、左房面積、左室駆出率、左室中隔壁厚、後壁壁厚を測定した。

- ・準備および血液、血行動態評価

ミダゾラム、セボフルラン、プロポフォールを使用し、挿管・人工呼吸器管理下に右頸静脈、左右大腿静脈、右大腿動脈にシースを留置した。採血を行い、血清インシュリン、レプチン、フォンウィルブランド因子、Dダイマーの測定を行った。解剖学的、電気的指標のために冠静脈洞にカテーテルを挿入した。心腔内超音波下に心房中隔穿刺を行い、左房へのアプローチを行った。血圧、左房圧の測定を行った

- ・電気生理学的検査

心房中隔穿刺後、左房へ SL-0 long シースを留置した。RAP を終了した際に、RAP 群、Obese-RAP 群すべて自然に洞調律へ復帰した。Ensite NavX システム下で、8極電極カテーテルを用いて右房、左房、肺静脈の三次元画像を構築し、同時に左房・肺静脈の局所電位を記録し voltage map を作成した。左房・肺静脈の局所電位は、左房中隔、後壁、左心耳、冠静脈洞、左右上肺静脈、下肺静脈で測定した。左房後壁、左心耳、右上、左上、下肺静脈において、基本心房刺激周期 400ms における有効不応期(Effective refractory period: ERP)を測定した。各部位 3 回ずつ測定を行い、平均値を解析に使用した。左心耳から 2、4、6、8、10 秒で高頻度心房刺激を行い、AF の持続時間 (1 秒以上) を測定し、最長の AF 持続時間を解析に使用した。

- ・組織学的検証

電気生理学的検査終了後、塩化カリウムの投与による安楽死を行い、心臓の組織学的検証を行った。Hematoxylin-Eosin 染色、Masson's Trichrome 染色を行った。右房はペースメーカーリードを留置していたこと、房室結節に焼灼を加えたことから組織学的検証は行わなかった。Masson's Trichrome 染色で線維化、脂肪浸潤の程度を、Hematoxylin-Eosin 染色で左房心筋細胞の肥大を評価した。この際、心外膜脂肪は心外膜と心筋との間にある脂肪組織として定義した。心房筋への脂肪浸潤は、心外膜から最大の脂肪浸潤までの距離を測定し、心房壁厚に対する比率を測定し%脂肪浸潤とした。%線維化は、心房筋全体における割合を



計測した。心房筋細胞の大きさは無作為に選択した 3 つの心房筋細胞の直径を測定し、平均値を解析に用いた。

#### ・遺伝学的検証

左房および左房-肺静脈接合部組織より TRIzol 試薬を用いて total RNA の抽出を行った。フィブロネクチン、コラーゲン I、コラーゲン III、TGF- $\beta$ 1 の評価を行った。

#### 【結果】

体重は、Obese-RAP 群、Obese 群でそれぞれ  $17.6 \pm 1.5$ kg、 $18.2 \pm 4.6$ kg であり、Control 群  $11.7 \pm 1.9$ kg、RAP 群  $10.7 \pm 1.4$ kg より高値を呈した。BCS は Obese-RAP 群、Obese 群でそれぞれ  $8.1 \pm 1.0/9$ 、 $7.5 \pm 1.0/9$  であり、Control 群  $5.2 \pm 0.8/9$ 、RAP 群  $5.1 \pm 1.5/9$  より有意に高値であった。拡張期血圧は、Control 群  $65.8 \pm 9.4$  mmHg、RAP 群  $67.4 \pm 11.5$  mmHg、Obese-RAP 群  $73.2 \pm 9.6$  mmHg、Obese 群  $88.2 \pm 13.3$ mmHg と Obese 群で有意に上昇していた。左房圧は、Control 群  $11.4 \pm 2.1$ mmHg、RAP 群  $11.9 \pm 6.4$ mmHg、Obese-RAP 群  $13.5 \pm 2.9$ mmHg、Obese 群  $23.4 \pm 6.9$ mmHg であり、Obese 群が有意に上昇していた。心腔内超音波指標には、4 群間に差を認めなかったが、Obese 群、Obese-RAP 群でインスリン濃度が Control 群、RAP 群より高値を呈した。(表 1) 高感度 CRP、中性脂肪はいずれの群でも上昇を認めなかった。

#### ・電気生理学的検査

電極カテーテルの近位電極と冠静脈洞遠位電極間の距離に基づいて計算された左房伝導速度は Control 群、RAP 群、Obese 群、Obese-RAP 群で有意差は見られなかった。全体の電位波高は Obese 群と比較し、Obese-RAP 群で有意に低かった(図 1)。ERP は、全体では各部位で Control 群、Obese 群、RAP 群と比較し、Obese-RAP 群が短縮する傾向があり、下肺静脈では有意に Control 群より RAP 群、Obese-RAP 群が短縮していた(RAP 群  $121.0 \pm 47.2$ ms、Obese-RAP 群  $122.0 \pm 37.0$ ms vs. コントロール群  $182.0 \pm 31.1$ ms,  $P=0.043$ )。高頻度連続刺激による AF 持続時間は、Control 群 0(0-0)秒、RAP 群 0(0-4.5)秒、Obese 群 2(0.5-2.8)秒、Obese-RAP 群 3(0-5.5)秒と段階的に延長した(図 2)。

#### ・組織学的検査

組織学的検証は、心外膜脂肪が Control 群、RAP 群、Obese 群、Obese-RAP 群で段階的に増加し、心房筋への脂肪浸潤も同様の傾向を認めた(心外膜脂肪の程度: Control 群  $93[41-79]$   $\mu$ m、RAP 群  $249[178-355]$   $\mu$ m、Obese 群  $233[136-329]$   $\mu$ m、Obese-RAP 群  $334[243-550]$   $\mu$ m、 $P<0.001$ ; %脂肪浸潤: Control 群  $7.3[0.7-17.1]$ %、RAP 群  $29.3[21.4-47.6]$ %、Obese 群  $27.9[12.5-31.7]$ %、Obese-RAP 群  $43.1[38.6-48.6]$ %、 $P<0.001$ ) (図 3)。%線維

化も僅かではあるが4群間で有意差を認め(Control群 1.5[0.6-1.9]%, RAP群 5.1[2.4-6.7]%, Obese群 1.4[0.8-2.6]%, Obese-RAP群 4.1[2.8-6.2]%,  $P=0.002$ )、RAP群、Obese-RAP群は他の2群と比較して大きかった(図4)。心房筋細胞のサイズは、Control群  $12.4 \pm 0.1 \mu\text{m}$ 、RAP群  $17.6 \pm 2.4 \mu\text{m}$ 、Obese群  $16.8 \pm 2.8 \mu\text{m}$ 、Obese-RAP群  $17.1 \pm 2.3 \mu\text{m}$  でControl群よりもRAP、Obese、Obese-RAP群で有意に大きかった(図3C)。心外膜脂肪の程度と脂肪浸潤率は左房、肺静脈での線維化と相関を認めた( $r=0.39$ ,  $P=0.001$ ;  $r=0.40$ ,  $P<0.001$ )。心外膜脂肪の厚さ、浸潤率と有効不応期の間に関係はみられなかったが、線維化の割合と有効不応期の間に関係を認めた( $r=-0.33$ ,  $P=0.004$ ) (図5)。

#### ・遺伝学的検証

分子生物学的検査において、線維化関連マーカーであるフィブロネクチン、I型、III型コラーゲン、TGF- $\beta$ 1のmRNA発現量は、Control群、Obese群では低いがRAP群、Obese-RAP群では増加しており、特にObese-RAP群ではControl群より有意に発現していた。フィブロネクチン1mRNAの発現がObese群と比較し、Obese-RAP群で有意に高値であった。そして、コラーゲンIIIのmRNA発現はObese-RAPとRAP群でObese群と比較し、有意に高値であった(図6)。

#### 【考察】

本研究は、AF単独、肥満単独、肥満合併AFによって促進される電気生理学的、構造的リモデリングの特徴を明らかにした。左房および肺静脈電位はObese群で最も高く、Obese-RAP群で最も低値であった。左房・肺静脈のERPは、下肺静脈ERPにおいて他の2群よりもRAP群とObese-RAP群で有意に短縮していた。高頻度刺激によって誘発されたAF持続時間は、Obese-RAP群およびObese群で他の2群と比較し、長かった。

#### ・肥満およびRAPによるAFモデルにおける心房筋リモデリング(肥満と心房細動の関連)

本研究では肥満犬モデルの作成を試みたが、実際にControl群およびRAP群よりもObese群およびObese-RAP群が高体重でBCSが高値を呈し外見的にも肥満であることから、肥満犬モデルの作成に成功したと言える。さらに肥満患者のAF合併を模擬したObese-RAPモデルは、世界で初めてのモデルであり、本研究で特出すべき点である。EPSでは、下肺静脈のERPがRAP群とObese-RAP群がControl群、Obese群に比較し短縮しており、Obese-RAPが最小値を呈した。ERP短縮は、心房伝導時間の延長と共に電気生理学的な心房筋リモデリングを反映する<sup>8</sup>。このような電気的リモデリングは心房細動の初期段階からみられると言われている<sup>8,9</sup>。したがって、電気的リモデリングは、AF単独を模擬したRAP群、Obese-RAP群両者でみられ、肥満合併AFモデルが最も亢進していることが示唆された。電位波高は、Obese-RAP群で他群に比較し、最も低値であった。さらに、線維化関連マーカーの発現がObese-RAP群、RAP群でみられた。AF発症の初期段階でみられる電気的

リモデリングは、AFが数か月に持続すると、心房線維化、心房筋の肥大および拡張をはじめとした構造リモデリングを引き起こす<sup>8</sup>。したがって、RAP群、Obese-RAP群両者には構造的リモデリングも生じていることが示唆される。本研究では肥満によって引き起こされる炎症または自律神経障害を裏付けるような明らかな所見はみられなかったが、拡張期血圧および左房圧はObese群で有意に増加していた。さらにObese群では心房筋細胞の肥大が見られ、AFの誘発性も僅かにみられた。これは、左房圧の上昇に伴う心房及び肺静脈のストレッチが関連していると考えられる。実験的に、急性心房進展により心房のERPが短縮し、心房の伝導速度を低下させ、ストレッチ活性化チャネルの開放による細胞興奮の低下がみられると報告されている<sup>10,11</sup>。また、肥満によって引き起こされる電気生理学的特性に関する臨床研究では、肥満患者の肺静脈のERPも短縮する傾向があることが示されている<sup>12</sup>。Obese群で見られたこれらの所見は、臨床的にみられる肥満患者の初期段階のリモデリングを反映していると考えられる。Obese-RAP群では、電氣的、構造的リモデリングが最大であることから、肥満に伴う血行動態的な変化がさらに心房筋リモデリングを促進する可能性があることを示している。

#### ・肥満と心外膜脂肪の関連

本研究では、心外膜脂肪量の程度と、脂肪浸潤はcontrol群と比較し、Obese群、Obese-RAP群で有意に大きくみられた。前述の通り、Control群およびRAP群よりもObese群およびObese-RAP群が高体重でBCSが高値を呈し外見的にも肥満であることから、肥満犬モデルの作成に成功したと言える。組織学的に、心外膜脂肪量と、心房筋への脂肪浸潤はObese、Obese-RAP群とともにControl、RAP群と比較し、大きかった。メタボリックシンドローム患者の心外膜脂肪量は非メタボリックシンドローム患者よりも有意に大きいことが知られており<sup>13</sup>、本研究でも同様の結果を得ることができた。肥満患者では中性脂肪や炎症マーカーが上昇することが知られているが、今回の研究ではいずれの群でも中性脂肪、高感度CRPの上昇はみられなかった。このことは、肥満モデル作成における高脂肪食投与期間や、ビーグル種を用いた影響が考えられる。

#### ・心房筋リモデリングにおける心外膜脂肪の役割（心外膜脂肪と心房細動の関連）

本研究では、心外膜脂肪と脂肪浸潤はObese群、Obese-RAP群のみならずRAP群でもみられた。開胸手術の際に左心耳切除を行った心房細動患者での研究でも心外膜脂肪が心房筋への浸潤を認めたことが報告されている<sup>14</sup>。したがって、AF単独の存在によっても心外膜脂肪と脂肪浸潤が引き起こされる可能性があることを改めて示した。心外膜脂肪がAFを引き起こす機序として、心外膜脂肪から放出される炎症性サイトカインによる隣接した心房筋への影響、心外膜脂肪に含まれるGPからの異常興奮や心臓周辺の心外膜脂肪の増加による直接圧迫による拡張障害の促進などの可能性が示唆されている<sup>6</sup>。本研究では、心外膜脂肪と脂肪浸潤は間質の線維化と相関を認めていることから、心房壁への脂肪浸潤

が線維化を引き起こす一要因であることが示唆された。しかし、線維化関連の mRNA 発現が RAP および Obese-RAP 群では観察されたが、Obese 群では見られなかった。ヒツジを用いた動物実験において、高脂肪食を 1 年間与えた肥満モデルでは、通常食を与えた対照群と比較し、有意な脂肪浸潤と線維性変化が認められている<sup>15</sup>。このことから、本研究での高脂肪食の餌付け期間が短かった可能性があると考えられる。以前に我々が報告した臨床研究では、左房周囲に存在する心外膜脂肪の局在は AF 維持に関連し伝導の不均一性を示す AF 中の分裂電位の局在と関連していた<sup>16</sup>。今回、脂肪浸潤と伝導の不均一性を反映する ERP 短縮との間に直接的な関連は見つからなかったが、組織内の線維化の割合は ERP 短縮と相関を認めた。このことから、心外膜脂肪、心房筋への脂肪浸潤は、線維化発現の律速因子として作用する可能性があることを示唆している。AF 発症維持の機序における心外膜脂肪の厚さおよび脂肪浸潤の役割は様々な可能性があるため、この点を明らかにするためにはさらなる研究が必要であると考えられる。

#### 【研究の限界】

第一に各群 5 頭の少数例での比較のため、統計的に有意差が出なかった可能性がある。第二に、肥満イヌモデルを作成するための最適な期間は確立されていない。組織学的変化を来たしうるには、さらに長期の肥満モデルが必要である可能性がある。第三に、日本では研究用の雄のビーグル犬を入手することが困難であったため、雌のみのビーグル犬を使用した。雌ビーグル犬は肥満傾向を呈する可能性が過去の報告で示されていることから、本研究の肥満モデルの体重増加に影響を与えていた可能性がある<sup>17</sup>。また、肥満の評価に BCS を使用したが、視覚的要素での評価は主観での項目であり、BCS のみでは確実な肥満の評価とはいえない可能性がある。第四に、今回分子学的解析には mRNA の解析を行ったが、タンパクレベルでの定量解析は、ビーグル犬を用いた実験では困難であり、評価を行えなかった。

#### 【結語】

肥満イヌモデルの左房圧は上昇し、電気生理学的に左房・肺静脈の電位波高が高値を呈し、短時間ながら心房細動誘発性を有した。組織学的には心外膜脂肪、脂肪浸潤の増加がみられた。これらは、肥満早期にみられる電気生理学的、組織学的特徴を反映している可能性がある。心房細動単独モデル、肥満合併心房細動モデルにおいては、電気生理学的に左房・肺静脈の ERP が短縮し、特に肥満合併心房細動モデルでは、心房細動誘発性が最大であった。これら両群における心外膜脂肪、脂肪浸潤は増加しており、これら組織学的変化が線維化の増加に関連していた。このことから、肥満や組織学的な心外膜脂肪や脂肪浸潤は、心房細動器質を規定する線維化を促進する律速因子である可能性を支持する重要な所見であると言える。しかしながら、依然として心外膜脂肪が心房細動に与える影響は様々な可能性が考えられ、さらなる研究が重要出る。実臨床においては、心房細動の治療に加え、日常生活を含

めた生活習慣の管理が心房細動治療において重要な因子となる可能性が考えられる。

## 【References】

1. Watanabe R, Nagashima K, Wakamatsu Y, Otsuka N, et al. Different Determinants of the Recurrence of Atrial Fibrillation and Adverse Clinical Events in the Mid-Term Period After Atrial Fibrillation Ablation. *Circulation journal*. 2021 Jul 3.doi:10.1253.
2. Monno K, Okumura Y, Saito Y, Aizawa Y, Nagashima K, Arai M, Watanabe R, Wakamatsu Y, Otsuka N, Yoda S, Hiro T, Watanabe I, Hirayama A. Effect of epicardial fat and metabolic syndrome on reverse atrial remodeling after ablation for atrial fibrillation. *J Arrhythm*. 2018;34:607-616.
3. Nagashima K, Okumura Y, Watanabe I, Nakai T, Ohkubo K, Kofune T, Kofune M, Mano H, Sonoda K, Hirayama A. Association between epicardial adipose tissue volumes on 3-dimensional reconstructed CT images and recurrence of atrial fibrillation after catheter ablation. *Circ J*. 2011;75:2559–2565.
4. Chung MK, Martin DO, Sprecher D, Wazni O, Kanderian A, Carnes CA, Bauer JA, Tchou PJ, Niebauer MJ, Natale A, Van Wagoner DR. C-reactive protein elevation in patients with atrial arrhythmias: inflammatory mechanisms and persistence of atrial fibrillation. *Circulation*.2001;104:2886–2891.
5. Iso K, Okumura Y, Watanabe I, Nagashima K, Takahashi K, Arai M, Watanabe R, Wakamatsu Y, Otsuka N, Yagyu S, Kurokawa S, Nakai T, Ohkubo K, Hirayama A. Is vagal response during left atrial ganglionated plexi stimulation a normal phenomenon?: comparison between patients with and without atrial fibrillation. *Circ Arrhythm Electrophysiol*. 2019;12:e007281.
6. Hatem SN, Redheuil A, Gandjbakhch E. Cardiac adipose tissue and atrial fibrillation: the perils of adiposity. *Cardiovasc Res*. 2014;102:205–213.
7. Liu DJX, Stock E, Broeckx BJG, Daminet S, Meyer E, Delanghe JR, Croubels S,

- Devreese M, Nguyen P, Bogaerts E, Hesta M, Vanderperren K. Weight-gain induced changes in renal perfusion assessed by contrast-enhanced ultrasound precede increases in urinary protein excretion suggestive of glomerular and tubular injury and normalize after weight-loss in dogs. *PLoS One*. 2020;15:e0231662.
8. Wijffels MC, Kirchhof CJ, Dorland R, Allessie MA. Atrial fibrillation begets atrial fibrillation. A study in awake chronically instrumented goats. *Circulation*. 1995;92:1954–1968.
  9. Allessie M, Ausma J, Schotten U. Electrical, contractile and structural remodeling during atrial fibrillation. *Cardiovasc Res*. 2002;54:230–246. Review.
  10. Ravelli F, Allessie M. Effects of atrial dilatation on refractory period and vulnerability to atrial fibrillation in the isolated Langendorff-perfused rabbit heart. *Circulation*. 1997;96:1686–1695.
  11. Bode F, Katchman A, Woosley RL, Franz MR. Gadolinium decreases stretch-induced vulnerability to atrial fibrillation. *Circulation*. 2000;101:2200–2205.
  12. Munger TM, Dong YX, Masaki M, Oh JK, Mankad SV, Borlaug BA, Asirvatham SJ, Shen WK, Lee HC, Bielinski SJ, Hodge DO, Herges RM, Buescher TL, Wu JH, Ma C, Zhang Y, Chen PS, Packer DL, Cha YM. Electrophysiological and hemodynamic characteristics associated with obesity in patients with atrial fibrillation. *J Am Coll Cardiol*. 2012;60:851–860.
  13. Balcioglu AS, Durakoglugil ME, Cicek D, Bal UA, Boyaci B, Muderrisoglu H. Epicardial adipose tissue and normal coronary arteries. *Diabetol Metab Syndr*. 2014;6:62.
  14. I Abe et al. Association of fibrotic remodeling and cytokines/chemokines content in epicardial adipose tissue with atrial myocardial fibrosis in patients with atrial fibrillation. *Heart Rhythm*. 2018;15:1717-727.
  15. Mahajan R, Lau DH, Brooks AG, Shipp NJ, Manavis J, Wood JP, Finnie JW, Samuel CS, Royce SG, Twomey DJ, Thanigaimani S, Kalman JM, Sanders P.

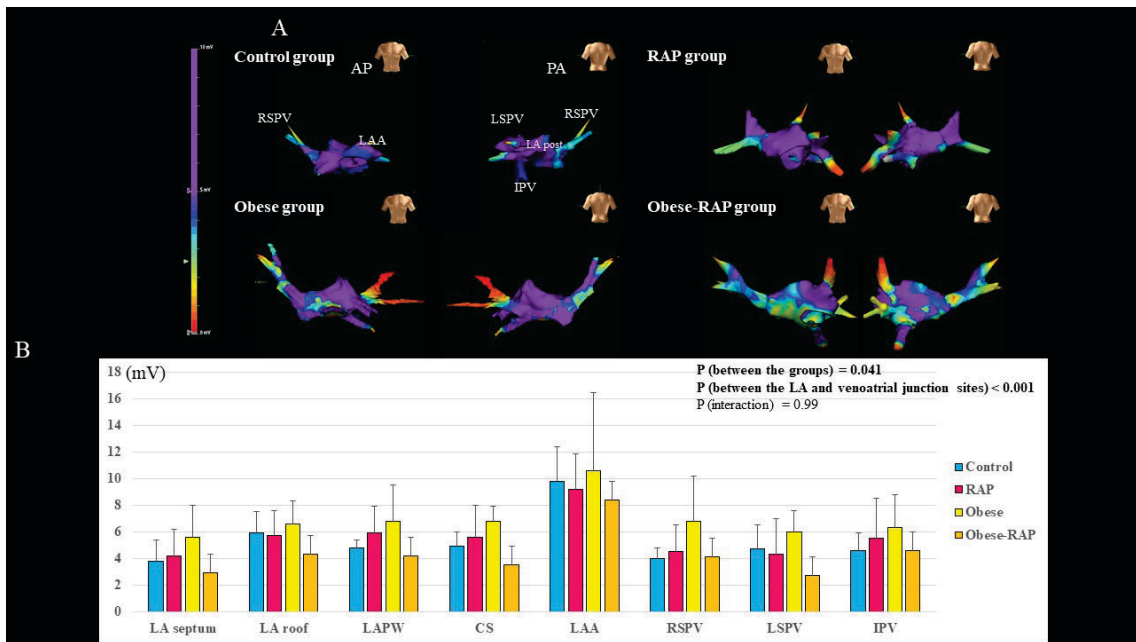
16. Electrophysiological, Electroanatomical, and Structural Remodeling of the Atria as Consequences of Sustained Obesity. *J Am Coll Cardiol.* 2015;66:1–11.
17. Nagashima K, Okumura Y, Watanabe I, Nakai T, Ohkubo K, Kofune M, Mano H, Sonoda K, Hiro T, Nikaido M, Hirayama A. Does location of epicardial adipose tissue correspond to endocardial high dominant frequency or complex fractionated atrial electrogram sites during atrial fibrillation? *Circ Arrhythm Electrophysiol.* 2012;5:676–683.
18. Usui S, Yasuda H, Koketsu Y. Characteristics of obese or overweight dogs visiting private Japanese veterinary clinics. *Asian Pac J Trop Biomed.* 2016;6:338–343.

表 1

	Control Group	RAP Group	Obese Group	Obese-RAP Group	<i>P</i> Value
Body weight (kg)	11.7±1.9	10.7±1.4	18.2±4.6*	17.6±1.5*	<0.001
Gained body weight (kg) by normal or high-fat diet	+2.6±1.1	+1.1±1.9	+7.1±3.5*	+6.6±1.5*	0.001
Body condition score	5.2±0.8/9	5.1±1.5/9	8.1±1.0/9	7.5±1.0/9	<0.001
Systolic BP (mmHg)	111.0±18.8	114.0±15.5	109.0±14.3	125.6±21.1	0.47
Diastolic BP (mmHg)	65.8±9.4	67.4±11.5	88.2±13.3*	73.2±9.6	0.02
LA pressure (mmHg)	11.4±2.1	11.9±6.4	23.4±6.9†	13.5±2.9	0.005
ICE measurements					
LA area (cm <sup>2</sup> )	5.6±1.3	3.8±2.0	5.4±1.3	5.7±1.5	0.23
IVSd (mm)	5.9±0.5	7.0±1.1	6.0±1.7	7.2±2.0	0.36
PWd (mm)	6.8±1.3	7.7±1.0	7.2±1.2	8.5±0.6	0.09
LVDd (mm)	25.7±4.0	24.1±5.8	26.2±4.4	20.8±4.4	0.30
LVEF (%)	70.2±5.6	63.6±14.7	60.6±6.1	69.6±13.7	0.46
Biomarker concentrations					
Insulin (mU/L)	6.9 (3.6–9.8)	5.7 (3.9–9.2)	14.4 (12.3–34.4)*	15.8 (9.1–55.4) ‡	0.012
Leptin (ng/mL)	0.9±0.4	0.7±0.2	1.0±0.2	0.8±0.3	0.35
vWF (%)	107±38	80±36	65±38	88±16	0.30
D-dimer (µg/mL)	0.27 (0.13–0.36)	0.35 (0.26–0.79)	0.25 (0.12–0.61)	0.48 (0.40–0.56)	0.09



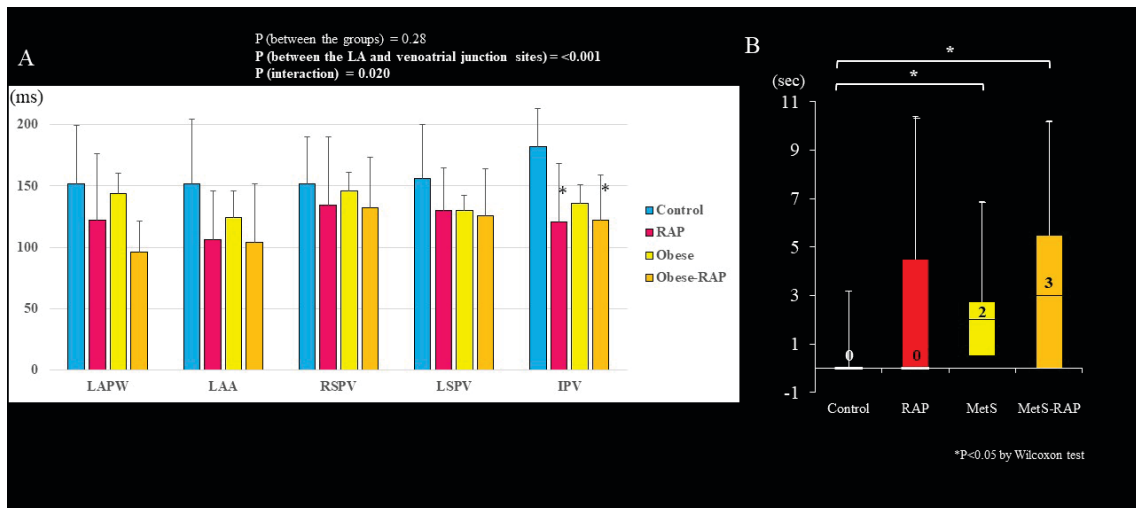
図 1



電気生理学的検査所見

A) 左房、肺静脈での 3D voltage map、B) 左房、静脈接合部での電位波高

図 2

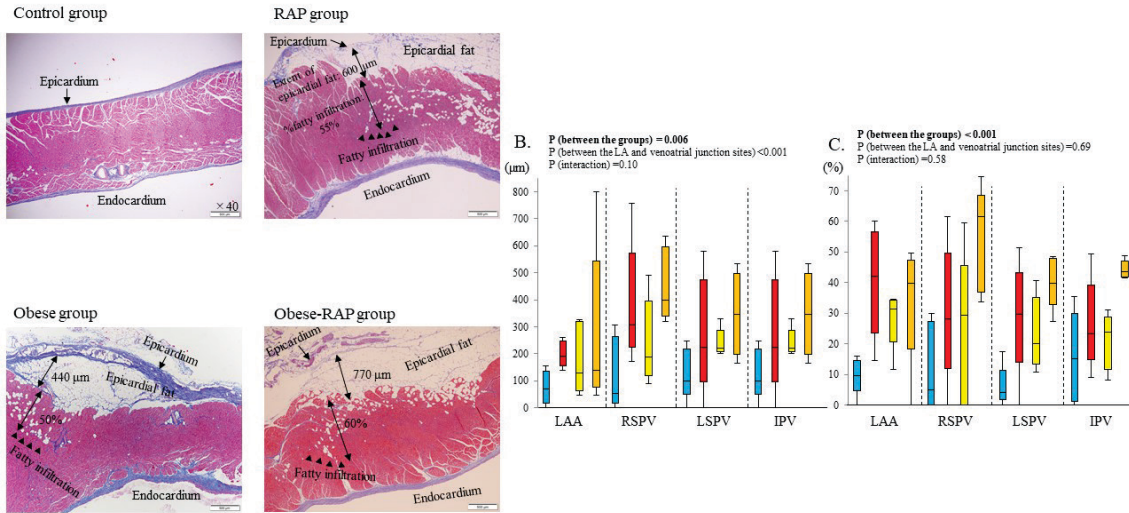


電気生理学的所見

A) 左房、静脈接合部での有効不応期、B) 心房高頻度刺激による心房細動持続時間

図 3

A.

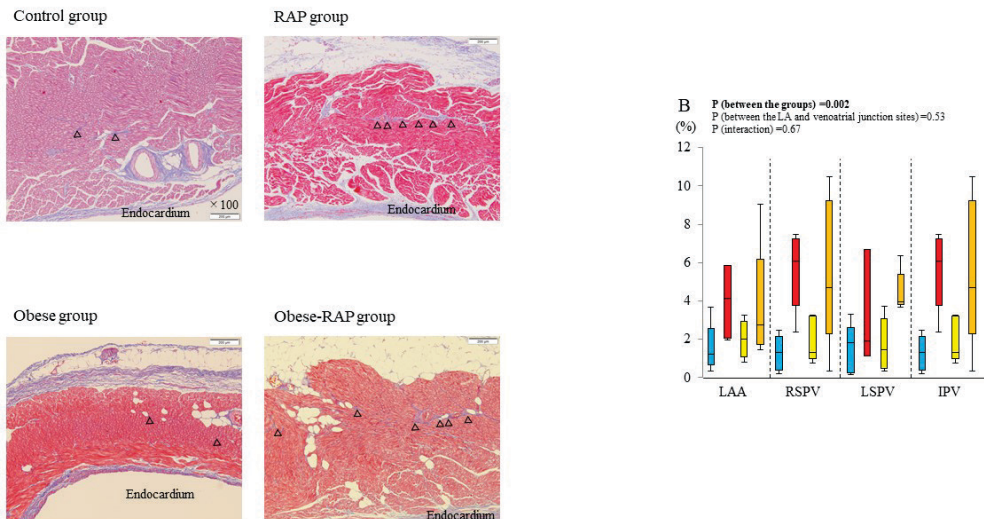


組織学的所見

- A) 左房肺静脈接合部の Masson's Trichrome 染色、B) 各部位での心外膜脂肪の程度、  
C) 各部位での心筋への%脂肪浸潤

図 4

A.

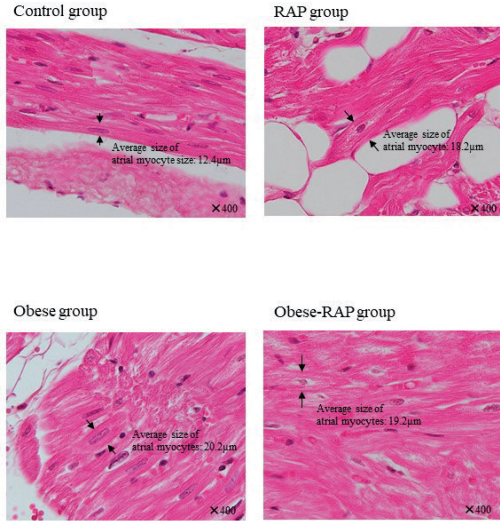


組織学的所見

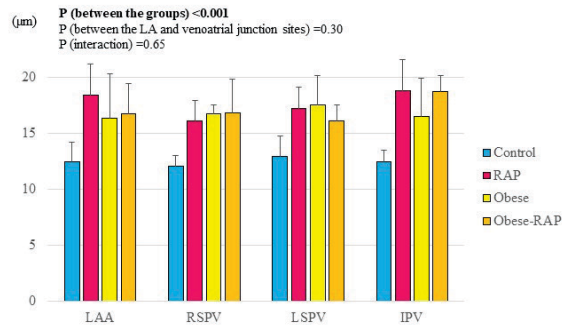
- A) 左房肺静脈接合部の Masson's Trichrome 染色、B) 各部位での%線維化

図 5

A.



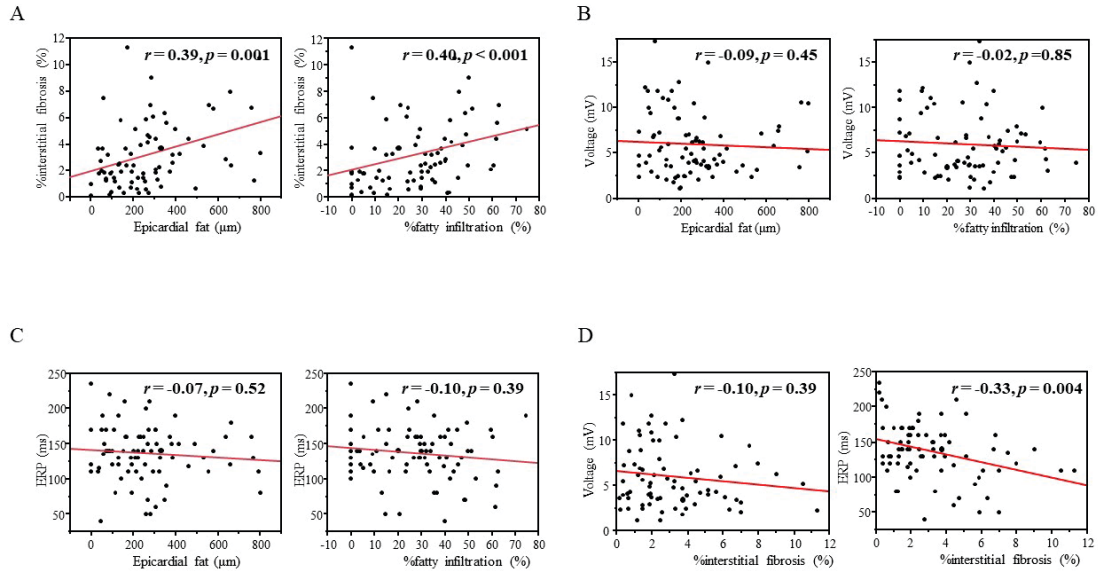
B.



組織学的所見

A) 左房肺静脈接合部の Hematoxylin-Eosin 染色、B) 各部位での心筋細胞サイズ

図 6

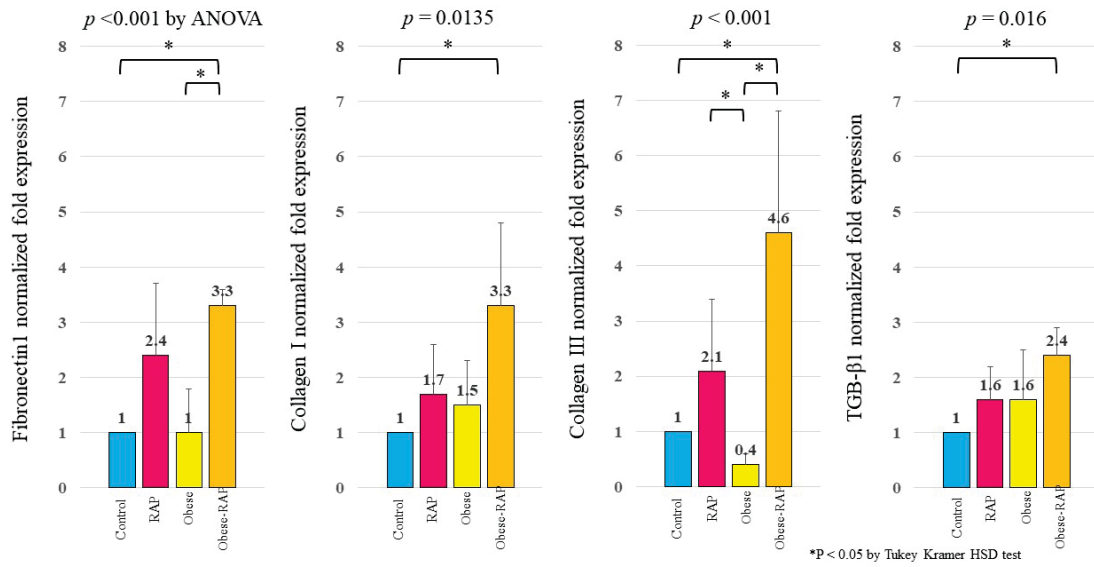


相関関係を示す散布図

A) %線維化と心外膜脂肪の程度、%脂肪浸潤の相関、B) 電位波高と心外膜脂肪、%脂肪浸潤の相関、C) 有効不応期と心外膜脂肪の程度、%脂肪浸潤の相関、D) 電位波高と%線

維化、有効不応期と%線維化の相関

図 7



各群における線維化関連 mRNA 表現マーカーの比較